University of Alberta

Characterization of a potential hepatic lipase, arylacetamide deacetylase (AADA)

by

Vivien Lo

A thesis submitted to the Faculty of Graduate Studies and Research
in partial fulfillment of the requirements for the degree of

Master of Science

Department of Cell Biology

Edmonton, Alberta
Fall, 2008

Library and
Archives Canada

Published Heritage
Branch

395 Wellington Street
Ottawa ON K1A 0N4
Canada

Bibliothèque et
Archives Canada

Direction du
Patrimoine de l'édition

395, rue Wellington
Ottawa ON K1A 0N4
Canada

Canada

Dedication

This thesis is dedicated to my future child/children

Life is a never-ending learning process. May the pursuit of knowledge bring you wisdom, and may the wisdom bring you happiness and success in life.

Abstract

Hydrolysis of hepatic intracellular triacylglycerol (TG) stores by lipases generates fatty acid substrates for the assembly of very low density lipoproteins (VLDL) and fatty acid oxidation. The identities of hepatic lipases are unknown, and arylacetamide deacetylase (AADA) is one of the candidate hepatic lipases. AADA is primarily expressed in liver and small intestine, and has sequence homology with the adipose tissue lipase, hormone sensitive lipase (HSL). AADA is 50 kDa N-linked glycosylated type II transmembrane protein localized to the ER, which is a subcellular compartment active in lipid synthesis and metabolism. Its transmembrane domain alone is sufficient for ER retention, but additional factors exist to enhance its ER localization. Expression of mouse AADA cDNA in McArdle RH7777 rat hepatoma (McA) cells significantly reduced intracellular TG levels. Moreover, this increase in intracellular TG turnover led to decreased secretion of apoB-associated TG, but increased fatty acid oxidation. This study demonstrates that AADA plays a role in hepatic lipid metabolism and expression in McA cells does not promote VLDL assembly but fatty acid oxidation.

Table of Contents

List of Tables

List of Figures

List of Abbreviations

4-MU	4-methylumbelliferone
4-MUH	4-methylumbelliferylheptanoate
AADA	Arylacetamide Deacetylase
Acyl-CoA	Acyl Coenzyme A
AGPAT	1-acylglycerol-3-phosphate acyltransferase
ApoB	Apolipoprotein B
ASM	Acid Soluble Metabolites
ATGL	Adipose Triglyceride Lipase
BSA	Bovine serum albumin
Cab-O-Sil	Fumed Silica
cAMP	Cyclic adenosine monophosphate
cDNA	Complementary deoxyribonucleic acid
CE	Cholesteryl ester
CHAPS	3-[(3-Cholamidopropyl)dimethylammonio]-1-propane-sulfonate
Ci	Curie
dpm	Disintegrations per minute
DG	Diacylglycerol
DGAT	Acyl-CoA:diacylglycerol acyltransferase
DMEM	Dulbecco's Modified Eagle's Medium
E600	Diethyl-p-nitrophenyl phosphate
EDTA	Ethylenediaminetetraacetic acid
eGFP	Enhanced green fluorescence protein

Endo H	Endoglycosidase H
ER	Endoplasmic reticulum
FBS	Fetal bovine serum
FP-biotin	6-N-Biotinylaminohexyl Isopropyl Phosphorofluoridate
g	Relative centrifugal force
G-418	Geneticin antibiotic
GC	Gas chromatography
GPAT	Glycerol-3-phosphate acyltransferase
HCl	Hydrochloric acid
HDL	High density lipoprotein
HRP	Horse radish peroxidase
HS	Horse serum
HSL	Hormone sensitive lipase
hTGH	Human triacylglycerol hydrolase
IDL	Intermediate density lipoprotein
KLH	Keyhole limpet hemocyanin
LDL	Low density lipoprotein
McA	McArdle RH7777 rat hepatoma
MG	Monoacylglycerol
MGAT	Acyl-CoA:monoacylglycerol acyltransferase
mRNA	Messenger ribonucleic acid
MTP	Microsomal triglyceride transfer protein
OA	Oleic acid

PA	Phosphatidic acid
PAP	Phosphatidic acid phosphohydrolase
PBS	Phosphate buffered saline
PC	Phosphatidylcholine
PCR	Polymerase chain reaction
PDI	Protein disulfide isomerase
PKA	Phosphokinase A
PL	Phospholipids
PL-C	Phospholipase C
PNGase F	Glycopeptidase F
pNp-acetate	*p*-nitrophenylacetate
pNp-OH	*p*-nitrophenol
rpm	Revolutions per minute
SDS-PAGE	Sodium dodecyl sulphate polyacrylamide gel electrophoresis
ST	Sialyltransferase
TBS	Tris-buffered saline
TCA	Trichloroacetic acid
TG	Triacylglycerol
TGH	Triacylglycerol hydrolase
TLC	Thin layer chromatography
TMD	Transmembrane domain
T-TBS	Tween 20-tris-buffered saline
VLDL	Very low density lipoprotein

CHAPTER 1

INTRODUCTION

1-1   Triacylglycerol metabolism

Triacylglycerol (TG) is the most concentrated and biologically inert form of energy available to biological tissues. Although most cells are capable of synthesizing TG, the adipose tissue and liver are the most important organs responsible for the storage of TG. Before the stored TG can be made available to tissues, it must undergo lipolysis, a process which requires the enzymatic activity of lipases to release fatty acids from TG. Due to the potent toxicity of elevated fatty acid levels, the regulation of TG metabolism is of utmost importance, and dysfunctions in the regulatory mechanisms are causes of many lipid metabolic disorders such as atherosclerosis, obesity and type II diabetes. TG, as well as phospholipids (PL), can be synthesized through the glycerol-3-phosphate pathway (Figure 1-1) (Coleman and Lee, 2004). The initial step involves conversion of glycerol or dihydroxyacetone-3-phosphate (DHAP) to glycerol-3-phosphate (G-3-P), which subsequently enters a rate-limiting reaction by acylation to form lysophosphatidate (LPA) by acyl-CoA: glycerol-*sn*-3-phosphate acyltransferase (GPAT) (Figure 1-1) (Coleman and Lee, 2004). Following acylation of LPA by acylglycerol-*sn*-3-phosphate acyltransferase (AGPAT) to form phosphatidic acid (PA), PA can be dephosphorylated by PA phosphohydrolase (PAPH) to liberate diacylglycerol (DG) (Coleman and Lee, 2004). DG is a critical intermediate for the synthesis of TG and PL, and different enzymes are responsible for the conversion of DG to various glycerolipids (Coleman and Lee, 2004). Since the synthesis of TG involves a complicated pathway, defects in the regulation of any step in the glycerolipid biosynthetic pathway will lead to alterations in neutral lipid levels and development of lipid metabolic disorders.
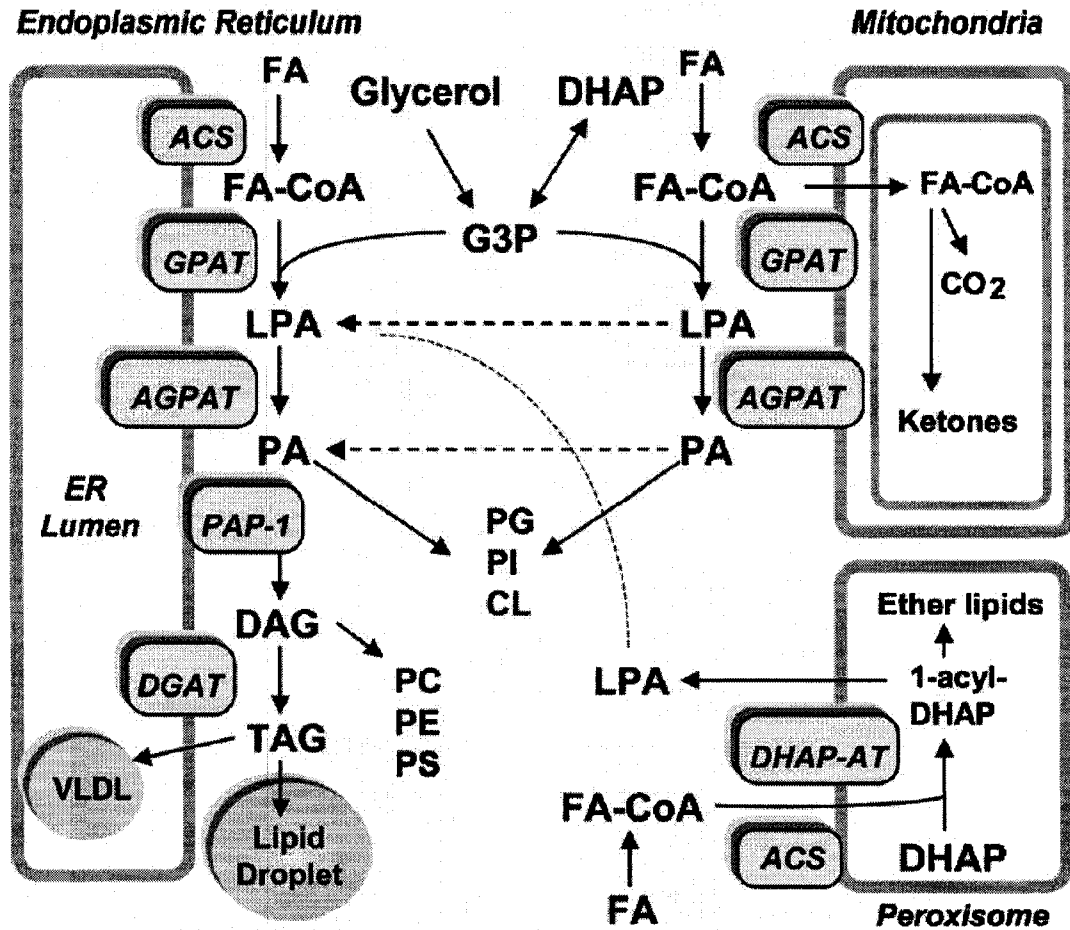
Figure 1-1. **Synthesis of triacylglycerol and its metabolic pathways.** ACS, acyl-CoA synthetase; AGPAT, acylglycerol-P acyltransferase; CL, cardiolipin; DAG, diacylglycerol; DGAT, diacylglycerol acyltransferase; DHAP, dihydroxyacetone-P; DHAP-AT, DHAP acyltransferase; ER, endoplasmic reticulum; FA, fatty acid; G3P, glycerol-3-P; GPAT, glycerol-P acyltrasnferase; LPA, lysophosphatidic acid; PA, phosphatidic acid; PAP, phosphatidic acid phosphohydrolase; PC, phoshatidylcholine; PE, phosphatidylethanolamine; PG, phosphatidylglycerol; PI, phosphatidylinositol; PLC, phospholipase C; PS, phosphatidylserine; TAG, triacylglycerol; VLDL, very low density lipoprotein. (Coleman and Lee, 2004)

3

1-2   Lipoproteins

Neutral lipids are insoluble in aqueous environment and must be transported in the circulation by lipoproteins, which are soluble complexes of proteins and lipids that transport lipids in blood. The different categories of lipoproteins are classified based on characteristics such as size, density, electrophoretic mobility, lipid contents and the lipid-binding apolipoproteins on the surface. The general structure of lipoproteins consists of a hydrophobic neutral lipid core rich in TG and cholesteryl esters (CE), and a hydrophilic surface monolayer that includes PL, cholesterol and apolipoproteins (Figure 1-2).

Chylomicrons are the largest class of lipoproteins with the highest TG content, and are therefore the least dense particles. These lipoproteins are secreted by the intestine to deliver dietary lipids to peripheral tissues in the post-prandial state. Very low density lipoproteins (VLDL) are the second largest class of lipoproteins that are also high in TG content, and each of these liver-derived particles contains a single molecule of apolipoprotein B (apoB). Other classes of lipoproteins include the intermediate density lipoproteins (IDL), low density lipoproteins (LDL), and high density lipoproteins (HDL), which have increasing density and decreasing particle size, respectively, as the TG content in the neutral lipid core decreases.

1-3   Assembly of very-low density lipoproteins (VLDL)

During the post-absorptive state, the liver secretes lipids into the circulation in the form of VLDL, which are utilized by peripheral tissues to meet energy demands. The assembly of VLDL involves both co-translational and post-translational addition of lipids

Phospholipids

Free cholesterol

Hydrophobic core

Exchangeable
apolipoprotein

Non-exchangeable
apolipoprotein
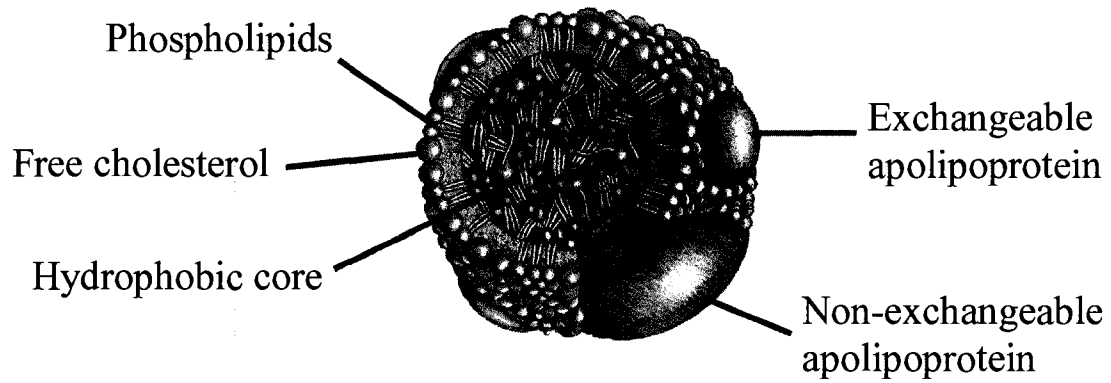
Figure 1-2. **The general structure of lipoprotein.** The hydrophilic surface monolayer consists of phospholipids, cholesterol and apolipoproteins; whereas the hydrophobic neutral lipid core consists of cholesteryl esters and triacylglycerol (Grundy, 1990).

to apoB (Boren *et al*, 1992; Rustaeus *et al*, 1998; Olofsson *et al*, 2000; Fisher *et al*, 2002). The transfer of lipids to nascent apoB particles is facilitated by the microsomal triglyceride transfer protein (MTP) (Yao *et al*, 1994; Mitchell *et al*, 1998) (Figure 1-3). MTP is also responsible for the formation of apoB-free endoplasmic reticulum (ER) lumenal lipid droplets (Raabe *et al*, 1999; Kulinski *et al*, 2002; Wang *et al*, 1999). These lipid droplets are believed to serve as lipid donors for bulk lipidation of primordial apoB-containing particles (Fisher *et al*, 2002; Wang *et al*, 2007) (Figure 1-3). An enzyme that has been implicated to play a role in the hydrolysis of stored TG pools and assembly of VLDL is a 60 kDa ER associated lipase, triacylglycerol hydrolase (TGH) (Dolinsky *et al*, 2004; Lehner and Verger, 1997; Lehner *et al*, 1999-A). Inhibition of TGH led to decreased TG mobilization and apoB secretion from hepatocytes (Gilham *et al*, 2003). However, treatment of hepatocytes with a TGH-specific inhibitor reduced secretion of TG and apoB to a lesser extent than did the general lipase inhibitor, diethyl-*p*-nitrophenyl phosphate (E600), suggesting that other lipases may also contribute to VLDL assembly (Gilham *et al*, 2003). The fact that perinatal rat hepatocytes are still capable of TG secretion in the absence of TGH expression in this particular developmental stage provides further support for the existence of additional lipases (Coleman *et al*, 1988; Lehner *et al*, 1999-B).

Cytosolic TG droplet
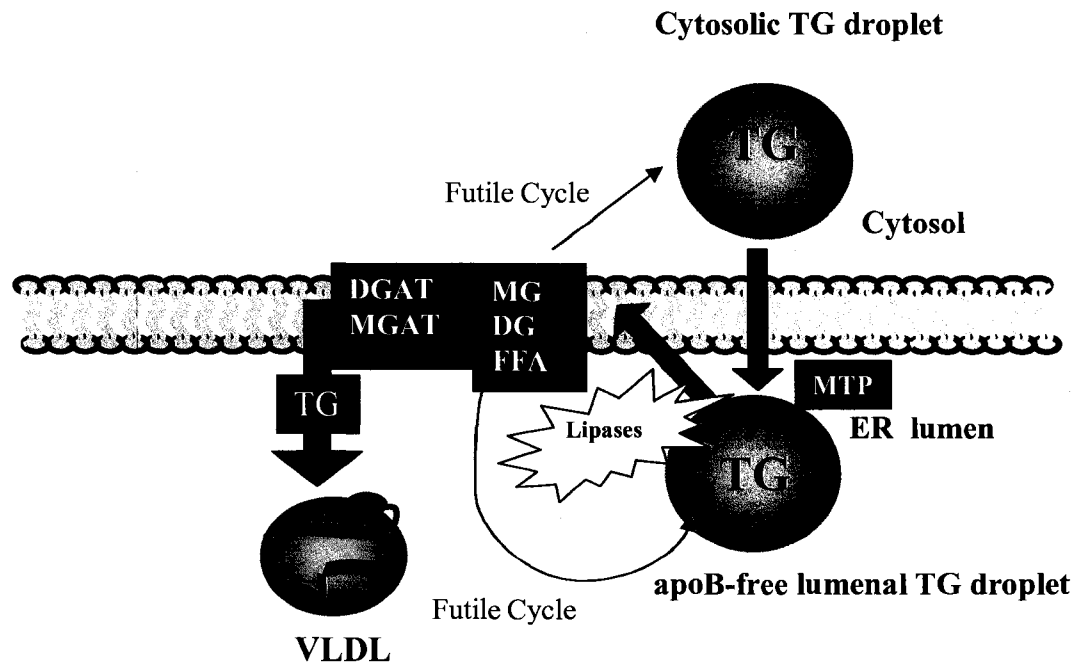
Figure 1-3. **The lipolysis and re-esterification cycle of TG for VLDL secretion.** Cytosolic TG is believed to be transferred into the ER lumen by microsomal triacylglycerol transfer protein (MTP), which is also responsible for the formation of apoB-free ER luminal TG droplets. These droplets are believed to serve as lipid donors for bulk lipidation of primordial apoB-containing particles to form VLDL particles. Prior to incorporation into VLDL, TG is first hydrolyzed by ER-associated lipases, and then re-esterified back to TG for the lipidation process. Alternatively, the re-esterified TG may be returned to cytosolic or luminal TG droplets in a futile cycle. ER = endoplasmic reticulum; FFA = free fatty acid; DG = diacylglycerol; MG = monoacylglycerol; TG = triacylglycerol; DGAT = diacylglycerol acyltransferase; MGAT = monoacylglycerol acyltransferase; VLDL = very low density lipoprotein

7

1-4 Mobilization of intracellular TG in liver

Hepatic TG stores provide a substrate for VLDL-TG following lipolysis and re-esterification (Francone *et al*, 1989). In addition, mobilization of intracellular TG stores can also provide substrates for the oxidative pathway leading to production of ketone bodies (Debeer *et al*, 1982). While there are major advances in the understanding of the contribution of lipolysis and re-esterification of intracellular TG stores to hepatic TG secretion, not much is known about how intracellular TG stores contribute to the oxidative pathway for ketogenesis.

In studies conducted by Wiggins *et al* (1992), the authors determined the percentages of secreted VLDL TG that arose from lipolysis of intracellular TG and that from en bloc secretion by comparing changes in the specific radioactivity of cellular TG pre-labeled with $[^{14}C]$glycerol and $[^{3}H]$oleate over a 24 hour chase period. From those experiments, the authors suggested that a 70 % loss of specific radioactivity in the ^{14}C-label in VLDL TG, although no change in ^{3}H-label, was a result of dilution of the $[^{14}C]$glycerol with unlabeled glycerol. This indicated that at least 70 % of VLDL TG was derived from lipolysis and re-esterification of intracellular TG, while at most 30 % was derived from intracellular TG that did not undergo lipolysis. The authors also claimed that a majority of the hydrolyzed TG was re-esterified and returned to the storage pools since the amount of TG hydrolyzed exceeded the amount required to maintain TG secretion (Wiggins, 1992). In addition, VLDL TG secretion was shown to be under hormonal regulation by insulin and glucagon. The secretion of VLDL TG was inhibited by insulin, and this was not a result of decreased en bloc TG secretion or decreased intracellular TG hydrolysis, but due to increased recycling back to the storage pools

(Wiggins *et al*, 1992). In contrast, glucagon resulted in an increase in lipolysis, but the fatty acids released were found to be destined for β-oxidation rather than for VLDL TG secretion (Wiggins *et al*, 1992). Besides changes in specific radioactivity, studies involving determination of the stereospecific distribution of fatty acids in the TG of liver and VLDL revealed that fatty acid compositions in the two forms of TG were different, which also supported the lipolysis and re-esterification phenomenon (Yang *et al*, 1995). Moreover, Lankester *et al* (1998) performed dual labeling studies with [^{3}H]oleate to distinguish fatty acids in endogenous stored TG from the [^{14}C]oleate-labeled exogenous fatty acids. The authors observed that exogenous [^{14}C]fatty acids contributed to only 17 % of total acyl chains secreted as TG, which indicated that most of the acyl chains in VLDL TG were derived from endogenous cytosolic TG stores. Gibbons *et al* (1992) have also shown that there is no relationship between extracellular fatty acid concentration and secretion of VLDL TG and apoB, but there is a dependence on the intracellular TG concentration. On the other hand, fatty acid oxidation depends largely on extracellular fatty acid concentration, and intracellular TG pool only has minor contributions (Gibbons, 1992). Although the intracellular TG pool was capable of providing substrates for fatty acid oxidation, this occurred mainly in the absence of extracellular fatty acids (Gibbons, 1992).

General agreement on the lipolysis and re-esterification model led to further investigation of whether specific hydrolytic products of intracellular TG are utilized for VLDL TG secretion. It has been postulated that if there were complete hydrolysis of intracellular TG to fatty acids and glycerol, both endogenously and exogenously derived fatty acids would be equally available for β-oxidation (Lankester *et al*, 1998). This

process is not efficient from an evolutionary perspective since it acts opposite to the enzymes within the phosphatidate pathway of TG synthesis. Indeed, observations on the positional distribution of specific acyl chains of TG in liver and VLDL indicated that there was almost complete identity between fatty acyl chains in the sn-1 and sn-2 positions, which provided evidence that intracellular TG was only partially hydrolyzed to diacylglycerols (DG) (Lankester *et* al, 1998), and to a smaller extent, monoacylglycerols (MG) (Yang *et al*, 1996). The fact that intracellular TG is not secreted en bloc but partially hydrolyzed and subsequently re-esterified to TG becomes a critical step to the regulation of hepatic TG secretion.

Treatment of hepatocytes with chloroquine, a lysosomal lipase inhibitor, did not result in changes in the overall amount of intracellular TG hydrolyzed and re-esterified (Wiggins, 1992). This led to the belief that lysosomal lipolysis has a relatively insignificant role in the lipolysis and re-esterification cycle, and TG lipases present in other subcellular compartments may be involved in the TG secretion and recycling pathway. Boren *et al* (1990) as well as other investigators have shown that apoB100, the main apolipoprotein associated with VLDL particles, is integrated into the membranes of ER. Since VLDL assembly takes place in the ER, a lipase that mobilizes intracellular stored TG would likely be located within the ER in order to divert lipolytic products for TG resynthesis and secretion.

Besides VLDL assembly, a small portion of fatty acids released from intracellular TG stores can also be utilized for energy production via β-oxidation in the mitochondria. Unlike the well-described roles of adipose triglyceride lipase (ATGL) and hormone-sensitive lipase (HSL) in the mobilization of TG stores in adipose tissue (Zimmermann *et*

al, 2004; Haemmerle *et al*, 2002; Holm *et al*, 2003; Hammerle *et al*, 2006; Kraemer *et al*, 2006), the identity of hepatic lipases supporting TG turnover, VLDL assembly and β-oxidation is still unclear.

1-5   Arylacetamide deacetylase, a potential hepatic lipase

Arylacetamide deacetylase (AADA) is a 50 kDa esterase that is primarily expressed in the liver and small intestine. The enzyme was first purified from human liver and characterized by Probst *et al* (1994). AADA was initially thought to be involved in activation of carcinogens by converting arylacetamide back to the carcinogenic primary arylamine compounds; however, carcinogenesis induced by primary arylamines is restricted to the bladder in which expression of AADA is not detected (Probst *et al*, 1994). Regardless of its possible role in xenobiotic metabolism, AADA was found to have properties that indicate a potential function in TG metabolism. First of all, there is a considerable sequence homology to HSL over a region spanning the characteristic lipase HGGG box and GXSXG active site motif, and another region comprising the catalytic triad of HSL (Probst *et al*, 1994). Secondly, AADA is primarily expressed in the liver and small intestine, which are organs active in TG metabolism (Probst *et al*, 1994). Thirdly, its lipase activity can be inhibited by organophosphates, which are potent lipase inhibitors (Trickett *et al*, 2001). In one study, Trickett *et al* (2001) have shown that hepatic AADA mRNA levels followed a diurnal rhythm with a pattern identical to hepatic VLDL secretion in mice. Additionally, preliminary results by Gibbons *et al.* (2000) suggested that HepG2 cells, a human hepatoma cell line deficient in mobilization of intracellular TG, transfected with AADA cDNA secreted more

preformed radiolabeled TG and fatty acids compared to control cells. Therefore, based on sequence homology to HSL and results claimed by Gibbons *et al* (2000), it is postulated that AADA may have a role in mobilization of hepatic intracellular TG to provide substrates for functions such as VLDL secretion or fatty acid oxidation.

The amino acid sequence of mouse AADA comprises a short N terminus, followed by a stretch of 17 hydrophobic residues predicted to be the transmembrane domain, and a potential glycosylation site at Asn 281 in the C terminus. Previous work with rabbit AADA implied microsomal membrane localization based on its presence in detergent-solubilized microsomes and the protein being glycosylated at both glycosylation sites at Asn 77 and Asn 281 (Ozols, 1998). These studies also revealed that the protein possesses a type II conformation with the N terminus facing the cytosol (Ozols, 1998).

Among soluble proteins that are targeted to the ER lumen, the most common targeting motif is the C-terminal KDEL sequence. Besides the consensus C-terminal KDEL sequence, other variants of this retrieval signal also exist such as the C-terminal HXEL sequence utilized by the soluble ER protein TGH (Robbi *et al*, 1991). While ER localization of soluble proteins depends largely on the KDEL receptor-mediated retrieval signals, formation of disulfide bonds between thiol-exposing proteins is another mechanism that has been identified (Anelli *et al*, 2002). Protein disulfide isomerase (PDI) is a protein that controls disulfide bond formation in the ER, and must be continuously re-oxidized, which is a process facilitated by the Ero1 family of proteins (Anelli *et al*, 2002). ERp44 is an ER luminal protein that mediates ER localization by forming mixed disulfide bonds with the unpaired cysteines in the Ero1 proteins as well as

some unassembled immunoglobulin subunits (Anelli *et al*, 2003). Although subcellular fractionation assays revealed that majority of ERp44 was found in the soluble fraction, a considerable portion was also found in the membrane pellet, suggesting that ERp44 may also interact with integral or peripheral membrane proteins (Anelli *et al*, 2002). However, the integral or peripheral membrane proteins that interact with ERp44 for thiol-mediated ER retention has not been identified. Unlike soluble ER proteins, the molecular signals responsible for insertion and retention of ER resident membrane proteins are still unclear. Some previous studies have demonstrated that two adjacent lysine residues located near the C-terminus represents a retrieval signal motif for type I ER membrane proteins (Jackson *et al*, 1990). In continuation with studies conducted by Jackson *et al* (1990), Schutze *et al* (1994) focused on the characterization of signals responsible for ER localization of type II integral membrane proteins. From these studies, it was shown that two adjacent arginine residues located in the N-terminal five amino acids are essential for targeting type II membrane proteins to the ER. While the proposed double-arginine motif is found in several type II ER membrane proteins, such targeting motif is absent from AADA.

In a separate study conducted by Mziaut *et al* (1999), the authors investigated the luminal targeting signals of two functionally unrelated ER luminal-oriented membrane proteins, 11β-hydroxysteroid dehydrogenase (11β-HSD) and esterase E3, another name for AADA. It was found that these two unrelated proteins share similar sequences in their N-terminus, but no resemblance in sequences beyond this segment (Mziaut, 1999). The two proteins share a short, positively charged N-terminus due to presence of an evolutionarily conserved lysine residue (region I), followed by a stretch of 17

hydrophobic residues containing an evolutionarily conserved tyrosine cluster (region II), and ending with two glutamate residues (region III) (Mziaut, 1999). Interestingly, although there is no functional relation between the two proteins, sequence similarities restricted to the N-terminus suggests that type II membrane topology signal exists within these short sequences. Therefore, the authors examined properties within the N-terminus that contribute to protein topology by generating various mutant GFP fusion constructs. Since deletion of the evolutionarily conserved tyrosine cluster resulted in the loss of membrane localization, the authors claimed that this region within the transmembrane domain is critical to membrane targeting and type II orientation of AADA. However, such deletion mutant may not represent a valid model since deletion of six residues in the transmembrane domain will result in a transmembrane segment that is too short for insertion into any membranes, hence the resultant cytosolic localization. In addition, all previous studies on AADA were performed with crude microsomal preparations that are not purified ER fractions and may also contain other subcellular organelles such as the Golgi. Therefore, the ER localization of AADA has not been conclusively determined and awaits confirmation.

Several factors that may determine specific protein topology including charge distribution in the anchor peptide and the length of the transmembrane domain have been proposed (Gafvelin, 1997). Although it is still unclear how AADA is retained in the membrane, it is postulated that AADA might be targeted to and restricted in the membrane by having a shorter transmembrane domain or formation of oligomers that prevent transport to the plasma membrane. Since insertion into cholesterol and sphingolipid-rich trans-Golgi and plasma membranes requires a transmembrane domain

of at least 23 residues in length, one that consists of 17 residues would not allow insertion into these thicker membranes (Munro, 1995). In addition, it is believed that interaction of the hydroxylated tyrosine residues within the transmembrane domain of AADA with the phospholipid headgroups would create an even shorter transmembrane helix than one that is composed entirely of hydrophobic residues (Gibbons *et al*, 2000).

The idea that protein retention can depend on transmembrane domain length is supported by studies performed by Munro (1995). In the study, Munro examined the retention mechanism of a trans-Golgi resident transmembrane protein, sialyltransferase (ST), by inserting additional amino acids to vary the length of its transmembrane domain, which also consists of 17 hydrophobic residues (Figure 1-4). As a result, the relative cell surface expression of the constructs increases as transmembrane domain length increases (Figure 1-4) (Munro, 1995). These findings are in agreement with the postulation that transmembrane domain length exhibits protein retention properties, and AADA may very likely utilize the same retention mechanism.

A

GDDD (DPPIV fusion)

MKTPWK⟨VLGLLGVAALVTIIIVPVVLL⟩KDEAAADSRRTYTLADYLgsknvtgskvf..

GSSS (ST fusion)

MIHTNLKKK⟨FSLFILVFLLFAVICVW⟩KKGSDYEALTLQAKEFQMgsknvtgskvf..

B

FSLFILVFLLFAVICVW
         ↘
1   V
2   VL
3   VAL
4   VLAL
5   VVLAL
6   ALVLAL
7   VALVLAL
8   VLALVLAL
9   VVLALVLAL

C
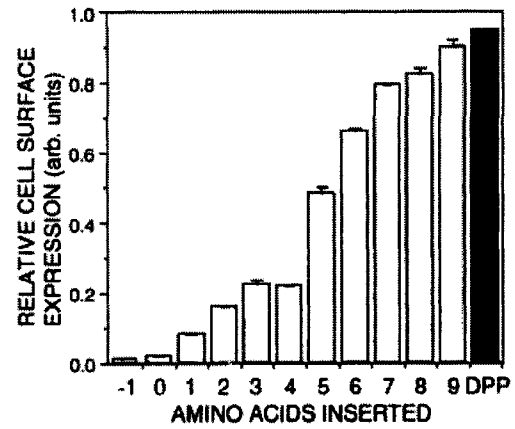
Figure 1-4. **Transmembrane domain length exhibits membrane retention properties.** The transmembrane domain of sialyltransferase (ST), a Golgi resident membrane protein, is replaced by transmembrane domains of various lengths. As the number of amino acid inserted increases, the relative cell surface expression of the resultant mutant construct increases (Munro, 1995).

16

1-6   Thesis objectives – localization and functional analysis of mouse AADA

The first objective was to study the precise subcellular localization and membrane retention mechanism of mouse AADA. Based on earlier studies, charge distribution (Mziaut *et al*, 1999) and transmembrane domain length (Munro, 1995) are the main determinants of protein localization and topology. It is therefore hypothesized that mouse AADA is localized to and retained in the ER by properties of the transmembrane domain, and mutations within this region can result in relocalization of the protein.   In order to test this hypothesis, two eGFP-tagged constructs, one with full-length AADA, and another with a transmembrane domain fragment (TMD) comprising the first 29 amino acids of AADA were generated. The purpose of generating the TMD-eGFP construct is to determine if the transmembrane domain of AADA alone is sufficient for membrane retention in its proposed location, the ER. In addition to wild type full-length AADA-eGFP and TMD-eGFP constructs, two mutants of both eGFP-tagged constructs bearing mutations within the transmembrane domain have also been generated by site-directed mutagenesis.   In the first set of mutations, the 3 polar tyrosine residues within the transmembrane domain were replaced by phenylalanine residues (Y-F mutation), which are structurally similar but non-polar residues. It is hypothesized if polarity, hence charge distribution, contributes to AADA retention, replacement of the tyrosine residues by phenylalanines will alter localization.   In the second set of mutations, 8 additional valine/leucine residues were inserted immediately after the valine residue at position 12 to generate a transmembrane domain with 25 residues (VL-insertion mutation), a length that is sufficient for insertion into thicker membranes such as the plasma membrane. It is hypothesized if AADA retention is based solely on the length of its transmembrane

domain, then an increase in transmembrane domain length will cause redistribution of AADA.

The second objective is to perform functional analysis of mouse AADA. Although very preliminary functional studies by Gibbons *et al* (2000) demonstrated that expression of human AADA in HepG2 cells resulted in a 3-fold increase in TG secretion, the effect of AADA expression on lipid turnover (lipolysis), intracellular lipid levels, apoB secretion and fatty acid oxidation has not been reported. In the present study, the potential role of AADA as a TG lipase and the subsequent fate of the hydrolyzed products are further investigated. The cell line model used for this study is a rat hepatoma cell line, McArdle RH7777 (McA), which is capable of secretion of newly synthesized TG but deficient in the mobilization of intracellular stored TG for VLDL assembly. As a result, two McA cell lines stably expressing mouse AADA cDNA have been established (cell lines A13 and A23) and metabolic labeling as well as lipid mass analyses were performed to address the role of AADA in hepatic lipid metabolism.

CHAPTER 2

MATERIALS AND METHODS

2-1   Materials:

Molecular biology reagents- all oligonucleotides were synthesized by Integrated DNA Technology (Coralville, IA). DNA sequencing was performed by the Molecular Biology Services Unit at the University of Alberta. All polymerase chain reactions (PCR) were performed in a PTC-200 Peltier Thermal Cycler from MJ Research, Inc. (Scarborough, ON). All restriction enzymes were purchased from New England Biolabs (Mississauga, ON). Trizol® Reagent, Lipofectamine 2000, T4 ligase, and all reagents required for PCR amplification including Taq DNA Polymerase, Platinum® Taq DNA Polymerase, DNAse I, oligo dT primers, deoxynucleotides triphosphates (dNTPs), SuperScript™ II reverse transcriptase and Platinum® SYBR®Green qPCR SuperMix-UDG were from Invitrogen (Burlington, ON).   Quikchange Site Directed-Mutagenesis Kit was purchased from Stratagene (La Jolla, CA).   The mammalian expression vector pCI-neo was from Promega Corporation (Madison, WI). The pEGFP-N1 vector was a kind gift from Dr. Sipione (University of Alberta).   All DNA plasmids were isolated from E. coli using QIAprep Spin Miniprep Kit or Endofree® Plasmid Maxi Kit from Qiagen (Mississauga, ON). Low Melt Agarose used for in-gel ligation was from BioRad (Mississauga, ON).

Chemicals- all organic solvents were obtained from Fisher Scientific (Ottawa, ON). 4-methylumbelliferylheptanoate (4-MUH), 4-methylumbelliferone sodium salt (4-MU), p-nitrophenyl acetate (pNP-acetate), taurodeoxycholate, lipid standards, phospholipase C (PL-C), anhydrous Na_2SO_4, essentially fatty acid-free bovine serum albumin (BSA), histodenz, pancreatin, Cab-O-Sil (fumed silica), oleic acid, paraformaldehyde and

diethyl-*p*-nitrophenyl phosphate (E600) were from Sigma (Oakville, ON). 6-N-biotinylaminohexyl isopropyl phosphorofluoridate (FP-biotin) was purchased from Toronto Research Chemicals (North York, ON). CytoScint scintillation fluid was from ICN Biomedicals (Irving, CA). Sylon BFT was from Supelco (Bellefonte, PA). 70 % perchloric acid was purchased from Anachemia (Edmonton, AB). En[3]hance™ Spray Surface Autoradiography Enhancer was purchased from Perkin Elmer (Waltham, MA). [9,10(n)-^{3}H]oleic acid (7 Ci/mmol) and [1-^{14}C]oleoyl-Coenzyme A (54.0 mCi/mmol) were from Amersham Biosciences (Oakville, ON).

Other materials- Penicillin, streptomycin, horse serum (HS), fetal bovine serum (FBS), geneticin (G-418), Dulbecco's Modified Eagle's Medium (DMEM), Ultra Pure Tris and Prolong® Antifade Kit were all from Invitrogen (Burlington, ON). Collagen solution, fetuin, PNGase F, Endoglycosidase H, protein A sepharose®, ampicillin sodium salt and kanamycin monosulfate were from Sigma (Oakville, ON). Cultures dishes were from Corning (New York, NY). Black and clear Microtest 96-well assay plates and conical polypropylene tubes were from BD Falcon (Franklin Lakes, NJ). M2 anti-FLAG antibodies were from Stratagene (La Jolla, CA). Goat anti-apoB antibodies were from Chemicon (Temecula, CA). Rabbit anti-Calnexin antibodies were from Stressgen (Victoria, BC). Secondary goat anti-rabbit and goat anti-mouse antibodies conjugated to horseradish peroxidase (HRP) were from Pierce Biotechnology (Rockford, IL). Secondary goat anti-mouse antibodies conjugated to the fluorophore Alexa 488 and donkey anti-rabbit antibodies conjugated to the fluorophore Texas Red were from Invitrogen Molecular Probe (Burlington, ON). Forty % acrylamide solution and protein

assay reagent were from BioRad (Mississauga, ON). Western Blotting Detection Reagents were from Amersham Biosciences (Oakville, ON). BioMax MR film was from Eastman Kodak Company (New Haven, CT). Complete Protease Inhibitor Cocktail tablets were from Roche. Thin Layer Chromatography (TLC) plates were from Whatman (Florham Park, NJ).

2-2   General Methodology:

Cloning of the chimeric mouse AADA cDNA- Two oligonucleotides were synthesized by Integrated DNA Technology corresponding to the cDNA sequence of mouse AADA. The forward primer contained sequence of the coding region of the cDNA [5'-ATG GGG AAA ACC ATT TCT CTT CTC-3']. The reverse primer corresponded to the complementary strand [5'-TTA CAG ATT TTT GAT AAG CCA ACT CAA-3']. These primers were used to amplify the AADA cDNA (~1.2 kb) from a mouse liver λgt11 cDNA library using *Pwo* polymerase (Roche). Amplification was performed at 93 °C for 1 min, 60 °C for 1 min and 72 °C for 2 min for 30 cycles. The PCR product was ligated into the *EcoRV* site of pBluescript II SK- plasmid (Stratagene) and the entire cDNA was sequenced. This plasmid was used as a template to generate a chimeric cDNA encoding the mouse AADA protein with a FLAG epitope at the extreme C-terminus (AADA-FLAG). The forward primer for AADA-FLAG [5'-G CAG CTC GAG ATG GGG AAA ACC ATT TCT CTT CTC ATC TC -3'] contained sequence of the coding region of AADA and the *XhoI* restriction site (underlined). The reverse primer for AADA-FLAG [5'-T CAT TCT AGA TCA CTT ATC GTC GTC ATC CTT GTA

ATC CAG ATT TTT GAT AAG CCA ACT CAA GTA CTG-3'] corresponding to the complementary strand, introduced the FLAG sequence (bold) immediately before the stop codon and the *XbaI* restriction site (underlined) following it. AADA-FLAG was amplified with *Taq* polymerase (Invitrogen), cloned into the pCR4-TOPO plasmid (Invitrogen) and sequenced. The chimeric cDNA was excised from this plasmid using *XhoI* and *SpeI* and was ligated into *XhoI* and *XbaI* digested pCI-neo (Promega) mammalian expression vector.

Cell culture of McArdle cells- McA cells, obtained from American Type Culture Collection, were cultured in DMEM containing 50 U/mL penicillin/streptomycin, 10 % horse serum and 10 % fetal bovine serum at 37 °C in humidified air containing 5 % CO_2.

Generation and cell culture of McArdle cell lines stably expressing AADA-FLAG cDNA- Wild-type McA cells of ~70 % confluency in 60 mm culture dishes were transfected with a Lipofectamine reaction mixture that was a combination of 500 µL of serum-free DMEM containing 8 µg of DNA (empty vector pCI-neo or AADA-FLAG-pCIneo) and 500 µL of serum-free DMEM containing 20 µL of Lipofectamine 2000. Cells were transfected for 4 hours in serum-free DMEM and then grown in DMEM with 1.6 mg/mL G-418 for 5 days to select for neomycin resistance. Individual clones were isolated and analyzed for AADA-FLAG protein by Western blotting. Stable cell lines, A13 and A23, were thereafter maintained in DMEM containing 0.4 mg/mL G-418, 10 % horse serum and 10 % fetal bovine serum at 37 °C in humidified air containing 5 % CO_2.

Preparation of total cellular membranes- Cells from 100 mm culture dishes grown to ~70 % confluency were harvested into 2 mL of phosphate buffered saline (PBS; 137 mM NaCl, 2.7 mM KCl, 10mM Na_2HPO_4 and 2 mM KH_2PO_4). Cells were disrupted by sonication and spun at 2465 g for 5 min to remove cell debris. The supernatant was subjected to ultracentrifugation for 45min at 355,040 g to isolate total cell membranes. The supernatant was removed and the pellet was resuspended in appropriate buffers for subsequent analyses.

Preparation of cellular membranes- Cells from 100 mm culture dishes grown to ~70 % confluency were harvested into 2 mL of PBS. Cells were disrupted by sonication for 20 seconds and spun at 10,000 g for 10 min to isolate cell debris, nuclei and mitochondria (this spin will also isolate some heavy microsomal membranes). The supernatant was subjected to ultracentrifugation for 45 min at 355,040 g to isolate cellular membrane fractions. The supernatant was removed and the pellet was resuspended in appropriate buffers for subsequent analyses.

Protein assays- Protein concentrations were determined with Protein Assay Reagent (BioRad). An aliquot of each sample was diluted with 200 μL of the Protein Assay Reagent and the final volume adjusted to 1 mL with H_2O. Protein concentration readings were performed in a BioRad SmartSpec™ 3000 at an absorbance of 595 nm.

Demonstration of esterase activity by activity-based probe FP-biotin- McArdle pCI-neo, A13, A23 and WT-hTGH cells were grown to ~70 % confluency in 100 mm

culture dishes and then harvested into 2 mL of PBS. Cells were disrupted by sonication for 20 seconds and 30 μg of total cellular proteins were treated with 1 % FP-biotin in 0.07 % Triton X-100 and incubated at room temperature for 30 min. Samples were then boiled for 5 min in 1X SDS-PAGE loading buffer (50 mM Tris, pH 6.8, 2 % SDS, 10 % glycerol, 10 % β-mercaptoethanol, 0.1 % Bromophenol Blue) and resolved in sodium dodecyl sulphate 10 % polyacrylamide gel (SDS-PAGE). Proteins were transferred to nitrocellulose membrane at 200 mAmp for 2 hours and blocked in 5 % skim milk for 45 min. Biotinylated proteins were detected by probing with streptavidin-HRP (BioRad) at 1:2000 dilution for 30 min and visualized by ECL.

In vitro esterase/lipase activity assays- Lipase and esterase activities in membrane fractions isolated from pCI-neo and AADA-FLAG stable cell lines were determined by measuring the hydrolysis of 4-MUH and pNP-acetate (Gilham and Lehner, 2005). Lipase activity against 4-MUH: 20 μg of total cellular proteins from McA cells expressing pCI-neo, A13 and A23 resuspended in assay buffer (20 mM Tris pH 8.0, 1 mM EDTA and 300 μM taurodeoxycholate) were incubated with 100 μM of the artificial fluorogenic 4-MUH substrate. A stock of 100 mM 4-MUH was made in tetrahydrofuran and was diluted with assay buffer prior to the experiment. The hydrolysis rate of 4-MUH was monitored by Fluoroskan Ascent Fluorimeter over a time course of 20 min. Esterase activity against pNP-acetate: 20 μg of total cellular proteins from McArdle cells expressing pCI-neo, A13 and A23 resuspended in assay buffer (20 mM Tris pH 8.0, 150 mM NaCl, 0.05 % Triton-X-100) were incubated with 100 μM pNP-acetate in the same assay buffer. A 20 mM stock of pNP-acetate was prepared in dichloromethane and

subsequently diluted with assay buffer to reach 100 μM. The hydrolysis of pNP-acetate

was monitored at 5 min intervals over a time course of 30 min at an absorbance of 405

nm using a BioRad SmartSpec™3000. Human triacylglycerol hydrolase (TGH) in serum

free DMEM was used as a positive control for both pNP-acetate and 4-MUH assays

(Gilham *et al*, 2005; Alam *et al*, 2006).

Preparation of 10 mM OA/ 10 % BSA complex- Sixty mg of oleic acid (Sigma

Cat. No. O-3879) were dissolved in 2 mL of 100 % ethanol, then neutralized by addition

of 100 μL of 5 M NaOH. The sodium oleate precipitate was dried down under nitrogen

for 10 min and then dissolved in 10 mL of 150 mM NaCl by warming to 60 °C. Once

temperature was reached, 10 mL of 20 % albumin in 150 mM NaCl were added to the

warm sodium oleate solution. The solution was stirred at room temperature for 10 min

and then stored in aliquots at -20 °C.

Metabolic labeling studies- McArdle pCI-neo, A13 and A23 cell lines were

grown to ~70 % confluency in 60 mm culture dishes. Cells were pulsed for 4 hours with

2 mL of serum-free DMEM containing 0.4 mM oleic acid (OA) complexed to 0.4 % BSA

and 2.5 μCi/mL of [9,10(n)-^{3}H]OA to stimulate neutral lipid synthesis. Some dishes from

each cell line contained 100 μM E600 to inhibit lipase activity. After 4 hour pulse, some

cells and media were collected for analyses. For the remaining cells, the pulse media

were aspirated, cells were washed 3 times with serum-free DMEM containing 0.4 % fatty

acid free BSA, then incubated with 2 mL of serum-free DMEM for an additional 4 hours,

which represented the 4 hour chase period. Some dishes from each cell line were also

incubated in the presence of 100 μM E600 to inhibit lipase activity. After 4 hour chase, cells and media were collected for analyses as described above. The pulse or chase media were centrifuged at 2465 g for 5 min to remove cell debris. All cells were washed with ice-cold PBS, harvested in the same buffer, and disrupted by sonication. One mL of cellular and media lipids from each sample was extracted by adding 4 mL of chloroform/methanol 2:1 containing lipid carriers and a drop of 1 M HCl (Folch et al, 1957). The lower organic phase was isolated, dried under nitrogen gas and then re-dissolved in 25 μL of chloroform. The lipid samples were spotted on thin-layer chromatography (TLC) plates and resolved in a phospholipids solvent system (chloroform/methanol/acetic acid/water 500:300:80:40) followed by a neutral lipids solvent system (heptane/isopropyl ether/acetic acid 600:400:40) before visualization by exposure to iodine (Gilham et al, 2003). Triacylglycerol (TG), cholesteryl ester (CE) and phosphatidylcholine (PC) were recovered and their radioactive contents were determined by scintillation counting.

Measurement of lipid synthesis by labeling studies- McArdle pCI-neo, A13 and A23 cell lines were grown to ~70 % confluency in 60 mm culture dishes. Cells were incubated with 2 mL of serum-free DMEM containing 2.5 μCi/mL of [9, 10(n)-^{3}H]OA and 0.4 mM OA complexed to 0.4 % BSA for 15, 30, 45 and 60 min. Cells were washed with ice-cold PBS, harvested in 2 mL of the same buffer and disrupted by sonication. Lipids were extracted from 1 mL of cell lysates by addition of 4 mL of chloroform/methanol 2:1 containing lipid carriers and a drop of 1 M HCl (Folch et al, 1957). The remaining procedures were identical to the previous descriptions in

Metabolic labeling studies. Radioactivity incorporation into TG and PC were measured by scintillation counting.

Measurement of fatty acid uptake by labeling studies- McArdle pCI-neo, A13 and A23 cell lines were grown to ~70 % confluency in 60 mm culture dishes. Cells were incubated with 2 mL of serum-free DMEM containing 2.5 μCi/mL of [9,10(n)-^{3}H]OA and 0.4 mM OA complexed to 0.4 % BSA for 15, 30, 45 and 60 min. Cells were washed with 0.4 % BSA in ice-cold PBS, harvested in 2 mL of PBS and disrupted by sonication. An aliquot of the total cell lysate was removed and the amount of radioactive fatty acid taken up was determined by scintillation counting.

Measurements of oleic acid incorporation into cellular lipids- McArdle pCI-neo, A13 and A23 cell lines were grown to ~70 % confluency in 60 mm culture dishes. Cells were incubated for 4 hours with 2 mL of serum-free DMEM containing 0.4 mM OA complexed to 0.4 % BSA in the presence or absence of 100 μM E600. After 4 hour OA loading, cells were washed with ice-cold PBS, harvested in 2 mL of the same buffer, and disrupted by sonication. 1 mL of cell lysates from each sample was incubated with
0.4 mL of 10X PL-C solution (10 U/mL PL-C, 175 mM Tris-HCl, pH 7.5, 100 mM CaCl$_2$), 0.6 mL of PBS and 2 mL of ether at 37 °C for 2 hours. The reaction was stopped by the addition of 1 mL of tridecanoin (2 μg/mL in chloroform) and 6 mL of chloroform/methanol 2:1 to the samples. The samples were mixed by vortexing and then centrifuged at 2465 g for 5 min. The lower organic phase was extracted and passed through a Pasteur pipet containing anhydrous Na$_2$SO$_4$. The samples were dried under

28

nitrogen and derivatized by incubating with 100 µL of Sylon BFT for 1 hour at room temperature. Following derivatization, the samples were dried under nitrogen and then re-dissolved in 100 µL of hexane. The total neutral lipids in the samples were measured by gas chromatography (GC). In this study, TG, CE and phospholipids (PL) were quantified.

Secretion of apoB- Media samples were collected at the end of 4 hour OA loading and then centrifuged at 2465 *g* for 5 min to isolate cell debris. For Cab-O-Sil precipitation, 60 µL of 50 mg/mL of Cab-O-Sil (fumed silica) resuspended in water was added to media samples with volumes equivalent to 0.5 mg of cell proteins and then adjusted to 1 mL with serum free DMEM. Samples were then incubated at 4 °C for 45 min and pelleted at 2465 *g* for 5 min. Samples were resuspended in 1X SDS-PAGE loading buffer (50 mM Tris, pH 6.8, 2 % SDS, 10 % Glycerol, 10 % β-mercaptoethanol, 0.1 % Bromophenol Blue) before proteins were boiled and resolved by BioRad 4-15 % Tris-HCl Ready Gels for 16 hours at 30 V and transferred to nitrocellulose membranes. Membranes were blocked with 5 % skim milk in Tris-buffered saline (TBS) containing 0.2 % Tween 20 (T-TBS) and were incubated with 1:5,000 goat anti-human apoB primary antibodies (Chemicon) followed by 1:10,000 HRP-mouse anti-goat secondary antibodies (Pierce). Immunoreactivity was detected by exposures to Biomax MR film (Kodak) after using ECL Western Blotting Detection Reagents. Secretion of albumin was used as a secretion control. After ECL detection, membranes were rinsed briefly with T-TBS and re-incubated with rabbit anti-rat albumin antibodies (gift from DE Vance Laboratory, University of Alberta) at 1:5000 dilution for 1 hour followed by goat anti-

rabbit-HRP secondary antibody incubation for 1 hour. ApoB band intensity was analyzed by Quantity One software (BioRad).

Fatty acid oxidation measurements- Cells grown to ~70 % confluency were incubated in 60 mm dishes with 2 mL of serum-free DMEM containing 0.4 mM OA complexed to 0.4 % BSA and 2.5 μCi/mL of [9,10(n)-³H]OA for 4 hours. At the end of the incubations, 30 μL of 20 % BSA and 16 μL of 70 % perchloric acid were added to culture media equivalent to 0.5 mg of cell proteins from each cell line. Culture media were centrifuged at 25,000 g for 5 min and an aliquot of the supernatant was counted for radioactivity. These experimental conditions were adapted from studies conducted by Hansson *et al* (2004).

In vitro hydrolysis of cellular membrane lipids derived from control and AADA-expressing McA cell lines- McArdle pCI-neo, A13 and A23 cell lines were grown to ~70 % confluency in 100 mm culture dishes. Cells were pulsed for 4 hours with 6 mL of serum-free DMEM containing 0.4 mM OA complexed to 0.4 % BSA and 2.5 μCi/mL of [9,10(n)-³H]OA to stimulate neutral lipid synthesis. At the end of the pulse incubation, cells were harvested in 2 mL of PBS and cellular membranes were prepared as described in *preparation of cellular membranes* in this chapter. Protein concentration was determined, and the maximum amount of membrane protein that could be used for each replicate was calculated based on the cell line with the lowest protein concentration. Sixty-eight μg of membrane proteins from McA pCI-neo, A13 and A23 cell lines were resuspended in 0.1 % BSA/PBS and incubated at 37°C for 0, 1 and 4 hours. As a positive

control, 10 μL of 50 μg/μL Pancreatin solution was added to separate samples containing McA pCI-neo membranes. At the end of the appropriate incubation times, lipids were extracted and separated by TLC as previously described. Following iodine staining of the TLC plates, the plates were sprayed 3 times with a thin coating of En^{3}hance™ Spray Surface Autoradiography Enhancer according to manufacturer's instructions. Once the plates were dried, they were wrapped in saran wrap and exposed to Biomax MR film (Kodak) at -80 °C for a week. The developed films were scanned and analyzed by densitometry using Quantity One software (BioRad).

In vitro oleoyl-CoA hydrolase assay- A 5 mM stock of oleoyl-CoA dissolved in water was diluted to 100 μM with 0.1 % CHAPS/PBS. 0.01 μCi/sample of [^{14}C]oleoyl-CoA was added and mixed with 10 μg of total cellular membrane proteins derived from McA pCI-neo and AADA cells in 0.1 % CHAPS/PBS. The reaction mixture was incubated for 30 min at 37 °C. The reaction was stopped by the addition of 4 mL of chloroform/methanol 2:1 containing lipid carriers, 800 μL of water and a drop of 1 M HCl in order to acidify the mixture for partitioning of fatty acids to the chloroform phase. The samples were mixed by vortexing and then centrifuged for 5 min at 2465 *g*. The chloroform phase was extracted, dried under nitrogen, resolved in 25 μL of chloroform, applied onto TLC plates, and resolved in organic solvents as described in the *metabolic labeling studies* section. The fatty acid bands were scraped into scintillation vials and the radioactivity contents were measured. As a positive control for the assay, 10 μL of 50 mg/mL of Pancreatin was added to a separate reaction mixture containing McA pCI-neo membranes.

In vitro diacylglycerol (DG) hydrolase assay- To prepare [9,10(n)-³H]oleate-labeled DG, a 100 mm dish of McA cells was incubated for 4 hours with 6 mL of serum-free DMEM containing 0.1 mM OA complexed to 0.1 % BSA and 5.0 µCi of [9,10(n)-³H]OA to stimulate neutral lipid synthesis. Cells were harvested in 1 mL of PBS and lipids extracted as described in the *metabolic labeling studies* section. After lipids were resolved in a neutral lipid solvent system, the origin containing all the phospholipids was scraped and transferred to a glass tube. Phospholipids were re-extracted from the silica by the addition of 4 mL of chloroform/methanol 2:1. After addition of 1 mL of water, the lower organic phase was extracted and dried under nitrogen. 1.8 mL of PBS, 0.2 mL of 10X PL-C solution (10 U/mL PL-C, 175 mM Tris-HCl, pH 7.5, 100 mM CaCl₂) and 2 mL of ether were added to the dried lipids and then incubated for 2 hours at 37 °C with vigorous shaking. 6 mL of choloroform/methanol 2:1 was added, followed by isolation of the lower organic phase and drying under nitrogen. The dried lipids were then resuspended in 1 mL of chloroform. An aliquot was taken to count the amount of radioactivity present in this substrate, and another aliquot was spotted on TLC plate to resolve DG, which should be the most prominent lipid.

Once the substrate radioactivity was determined, 0.01 µCi/sample was used for DG hydrolase assay. The assay contained [³H]DG re-dissolved in 20 µL of acetone and 90 µg of total cellular membrane proteins derived from McA pCI-neo and AADA cells in 0.1 % CHAPS/PBS. The total sample volume was adjusted to 200 µL with 0.1 % CHAPS/PBS. The reaction mixture was incubated for 30 min at 37 °C. After incubation, the assay proceeded in a similar fashion as the *in vitro oleoyl-CoA hydrolase assay*

described above. As a positive control for the assay, 10 μL of 50 mg/mL of Pancreatin was added to a separate reaction mixture containing McA pCI-neo membranes.

Generation of AADA polyclonal antibodies- Antibodies against mouse AADA were obtained by immunization of rabbits with the C-terminal 14 amino acids of mouse AADA linked to keyhole limpet hemocyanin (KLH). Briefly, rabbits were injected subcutaneously with an initial dose of 0.5 mg of the conjugated peptide in complete Freund's adjuvant followed by 3 booster injections of 0.2 mg of the conjugated peptide at 3 week intervals. Pre-immune and anti-AADA sera were prepared, aliquoted and stored at -80 °C.

Dot blot assay for determination of rabbit anti-AADA sera titre- Serial dilutions of pre-immune and anti-AADA sera were prepared at 1/33, 1/100, 1/330, 1/1000, 1/3300, 1/10,000, 1/33,000, 1/100,000, 1/330,000 with 3 % BSA in PBS. A nitrocellulose membrane was pre-incubated with 5 μg/mL of BSA-AADA peptide in PBS for 1 hour, rinsed with PBS 2 times for 5 min each, and then blocked with 3 % BSA in PBS for another hour. One μL of sera was spotted, well-spaced, on the nitrocellulose membrane. The membrane was incubated at room temperature for 30 min, rinsed 2 times with PBS for 5 min each, and then incubated with goat anti-rabbit-HRP at 1:10,000 dilution in 1 % BSA for 1 hour. After two 5 min washes with PBS, immunoreactivity was detected by addition of ECL reagents followed by exposure to Biomax MR films (Kodak).

Immunoblotting techniques- Protein samples were boiled for 5 min in 1X SDS-PAGE loading buffer (50 mM Tris, pH 6.8, 2 % SDS, 10 % Glycerol, 10 % β-mercaptoethanol, 0.1 % Bromophenol Blue), resolved by SDS-10 % PAGE, transferred to nitrocellulose and immunoblotted with the appropriate antibodies. All membranes were blocked with 5 % skim milk in Tween 20 tris-buffered saline (T-TBS; 0.1 % Tween 20, 20 mM Tris, pH 7.4, 137 mM NaCl) for 45 min prior to primary antibody incubations. All primary antibody incubations were carried out in 1 % skim milk solution in T-TBS for 1 hour. For monoclonal primary antibodies, mouse anti-FLAG antibodies (Stratagene) were used at 1:10,000 dilution, mouse anti-eGFP antibodies (gift from the Berthiaume Lab) were used at 1:10,000 dilution. After three 10 min washes with T-TBS, the membranes were incubated with 1:10,000 dilution of horseradish peroxidase (HRP)-conjugated goat anti-mouse secondary antibodies (Pierce). For polyclonal antibodies, incubations with rabbit anti-AADA sera were at 1:1000 dilution, with rabbit anti-rat TGH sera at 1:50,000 dilution, with rabbit anti-Calnexin (Stressgen) primary antibodies at 1:10,000 dilution, and with rabbit anti-TGN antibodies at 1:2000 dilution (gift from Dr. Hobman, University of Alberta). After three 10 min washes with T-TBS, the membranes were incubated with goat anti-rabbit-HRP secondary antibodies (Pierce) at 1:10,000 dilution. All immunoblots were exposed to BioMax MR films (Kodak) after using ECL Western Blotting Detection Reagents (Amersham Biosciences).

Glycopeptidase F (PNGase F) treatment – Cell lysates were prepared from A13 and TGH McA cell lines by homogenization in 100 mM Tris-HCl, pH 8.0. 10 µL of

10 % SDS, 10 μL of 10 % Triton X-100 and 2 μL of β-mercaptoethanol were added to 100 μL of cell lysates from A13 and TGH cell lines. Samples were boiled for 5 min and cooled on ice for 20 min. Half of each sample was treated with 2 μL (10 U) of PNGase F and the other half with 2 μL of Tris buffer (control). Samples were incubated overnight at 37 °C for deglycosylation, then boiled in 1X SDS-PAGE loading buffer and resolved by SDS-10 % PAGE. AADA and TGH were visualized by immunoblotting with anti-AADA and anti-TGH sera.

Endoglycosidase H (Endo H) treatment – Cell lysates were prepared from A13 and TGH McA cell lines by homogenization in TBS containing 2 % Triton X-100. 100 μL of 100 mM sodium citrate, pH 5.5, were added to 100 μL of cell lysates from A13 and TGH cell lines. Ten μL (50 mU) of Endo H were added to half of each sample and 10 μL of sodium citrate buffer (control) were added to the other half. Samples were incubated overnight at 37 °C for deglycosylation. Samples were boiled for 5 min in 1X SDS-PAGE loading buffer and resolved by SDS-10 % PAGE. AADA and TGH were visualized by immunoblotting with anti-AADA and anti-TGH sera.

Confocal immunofluorescence imaging of McArdle cells – Wild type McArdle cells or McArdle cells transfected with FLAG or various eGFP constructs were grown on glass coverslips in 6-well dishes with the appropriate medium overnight (see cell culture conditions in *Cell culture of McArdle cells, Generation and cell culture of McArdle cell lines stably expressing AADA-FLAG cDNA and Cloning and generation of transiently transfected McArdle cells expressing wild type and mutant eGFP-tagged constructs*). On

35

the next day, cells were fixed with 4 % paraformaldehyde in PBS for 10 min at room temperature, permeabilized with 0.2 % Triton X-100 in PBS for 5 min at room temperature and then subjected to antibody incubations. The primary antibodies used were: M2 anti-FLAG, mouse anti-eGFP (gift from Dr. Berthiaume, University of Alberta), rabbit anti-calnexin, rabbit anti-mannosidase II (gift from Dr. Hobman, University of Alberta), rabbit anti-sialyltransferase (gift from Dr. Hobman, University of Alberta), rabbit anti-TGN (gift from Dr. Hobman, University of Alberta), and rabbit anti-mouse AADA. The secondary antibodies used were: goat anti-rabbit Alexa 488, goat anti-mouse Alexa 488, donkey anti-rabbit Texas Red and donkey anti-mouse Texas Red. All primary and secondary antibody incubations were done at 1:100 dilution with 3 % BSA in PBS at 37 °C for 1 hour. After rinsing coverslips 3 times with PBS, they were mounted onto glass slides with Prolong ® Antifade Kit (Invitrogen) mounting medium and stored at 4 °C until the next day. All slides were viewed by a Zeiss LSM510 confocal microscope (Carl Zeiss Canada Ltd, Toronto, ON) using the Zeiss LSM510 Image Browser software at the facility in the Department of Cell Biology.

Confocal immunofluorescence imaging of mouse hepatocytes- Mouse hepatocytes isolated from wild type C57 BL/6J mouse were grown on collagen (Sigma) coated coverslips in 6-well dishes with DMEM containing 10 % HS and 10 % FBS overnight. On the next day, cells were fixed with 4 % paraformaldehyde in PBS for 10 min at room temperature, permeabilized with 0.2 % Triton X-100 in PBS for 5 min at room temperature and then subjected to antibody incubations. Cells were incubated with rabbit anti-AADA sera and mouse anti-PDI antibodies (Stressgen) at 1:100 dilution in 3 % BSA

in PBS for 1 hour. Samples were then incubated with goat anti-rabbit Alexa 488 and donkey anti-mouse Texas Red secondary antibodies at 1:100 dilution in 3 % BSA in PBS for 1 hour. After rinsing coverslips 3 times with PBS, the coverslips were mounted on glass slides with Prolong® Antifade Kit (Invitrogen) mounting medium and stored at 4 °C. All slides were viewed by a Zeiss LSM510 confocal microscope (Carl Zeiss Canada Ltd, Toronto, ON) using the Zeiss LSM510 Image Browser software at the facility in the Department of Cell Biology.

Subcellular fractionation- A liver harvested from wild type C57 BL/6J mouse was homogenized in ice-cold homogenizing buffer (10 mM Tris-HCl at pH 7.4, 250 mM sucrose, 5 mM EDTA and 1X complete protease inhibitor cocktail (Roche)). The homogenate was subjected to centrifugation at 10,000 g for 10 min to obtain post-nuclear supernatant. The remaining procedures were performed as described in Tran *et al* (2002): A Nycodenz gradient (Histodenz - Sigma) was pre-formed by loading in order from top to bottom, 2.5 mL of 10, 14.66, 19.33 and 24 % of a 27.6 % Nycodenz stock solution (in 10 mM Tris-HCl at pH 7.4, 3 mM KCl, 1 mM EDTA and 0.02 % NaN$_3$). The diluted Nycodenz solutions were prepared by diluting the 27.6 % stock solution with 0.75 % NaCl (in 10 mM Tris-HCl at pH 7.4, 3 mM KCl, 1 mM EDTA and 0.02 % NaN$_3$). The tube containing this Nycodenz gradient was then sealed with parafilm and placed horizontally at room temperature for 45 min and then centrifuged at 169,044 g for 4 hours at 15 °C in a SW41 rotor in order to create a non-linear gradient. Once the gradient was formed, the post-nuclear supernatant was applied on top of the gradient and then subjected to centrifugation at 169,044 g for 1.5 hour at 15 °C. After centrifugation,

fifteen 800 µL fractions were isolated from the gradient, and 160 µL from each fraction

was subjected to acetone precipitation by the addition of 640 µL of acetone (a volume

equivalent to 4 times the volume of the samples) and incubated for 1 hour at -20 °C. The

samples were spun at 13,000 g for 10 min to pellet the precipitated proteins. The

supernatant was removed and the pellets were resuspended in 50 µL of 1X SDS-PAGE

loading buffer, boiled for 5 min and then separated by 10 % SDS-PAGE. Proteins were

transferred to nitrocellulose membrane and the remaining procedures were as described in

immunoblotting techniques. Rabbit anti-TGN and rabbit anti-calnexin were used to detect

TGN and calnexin, which are subcellular markers for the Golgi and the ER, respectively.

*Generation of transiently transfected McArdle cells expressing wild type and

mutant eGFP-tagged constructs* – Two sets of eGFP constructs were designed and

generated by Quikchange Site Directed Mutagenesis Kit from Stratagene: wild type and

mutant AADA-eGFP, and wild type and mutant transmembrane domain (TMD) eGFP

constructs. Oligonucleotide primers used for the amplification of each construct are

listed in Table 2-1. The TMD fragment consists of the first 29 amino acids of AADA,

which includes a stretch of 17 hydrophobic residues forming the transmembrane domain

of the protein. In the first set of mutations, the 3 tyrosine residues at positions 16, 17 and

19 within the transmembrane domain were mutated to structurally similar phenylalanines.

This mutation was performed in both AADA-eGFP and TMD-eGFP constructs. In the

second set of mutations, 8 alternating valine and leucine residues were inserted into the

transmembrane domain in order to increase the length of the membrane-spanning

Table 2-1. Oligonucleotides used for the amplification of eGFP constructs.

Constructs	Primer sequences
AADA-eGFP forward	5'- GCG CGC GCA GAT CTA TGG GGA AAA CCA TTT CTC TT-3'
AADA-eGFP reverse	5'- CGC GCG CGC TGC AGC AGA TTT TTG ATA AGC CAA CTC-3'
VL-AADA-eGFP forward	5'-TCT CTT CTC ATC TCT GTG GTG GTT CTA GTG CTT GTG CTT GTC CTG CTT GTA GCT TAT TAT CTT TAT-3'
VL-AADA-eGFP reverse	5'- ATA AAG ATA ATA AGC TAC AAG CAG GAC AAG CAC AAG CAC TAG AAC CAC CAC AGA GAT GAG AAG AGA-3'
YF-AADA-eGFP forward	First Round: 5'- TCT CTG TGG TGA TTG TAG CTT ATT ATC TTT TCA TAC CGC TTC CAG ATG C-3' Second Round: 5'- CTC ATC TCT GTG GTG CTT GTA GCT TTC TTC CTT TTC ATA CCG CTT CCA GAT GC-3'
YF-AADA eGFP reverse	First Round: 5'-GCA TCT GGA AGC GGT ATG AAA AGA TAA TAA GCT ACA AGC ACC ACA GAG A-3' Second Round: 5'-ATG CAT CTG GAA GCG GTA TGA AAA GGA AGA AAG CTA CAA GCA CCA CAG AGA TGA G-3'
TMD-eGFP forward	5'- GCG CGC GCA GAT CTA TGG GGA AAA CCA TTT CTC TT-3'
TMD-eGFP reverse	5'- CGC GCG CGC TGC AGA GGT CTA CGA TAA CTT CTC GGA-3'
VL-TMD-eGFP forward	5'-TCT CTT CTC ATC TCT GTG GTG GTT CTA GTG CTT GTG CTT GTC CTG CTT GTA GCT TAT TAT CTT TAT-3'
VL-TMD-eGFP reverse	5'- ATA AAG ATA ATA AGC TAC AAG CAG GAC AAG CAC AAG CAC TAG AAC CAC CAC AGA GAT GAG AAG AGA-3'
YF-TMD-eGFP forward	5'- CAT CTC TGT GGT GCT TGT AGC TTT TTT TCT TTT TAT ACC GCT TCC AGA TGC TAT TG-3'
YF-TMD-eGFP reverse	5'- CAA TAG CAT CTG GAA GCG GTA TAA AAA GAA AAA AAG CTA CAA GCA CCA CAG AGA TG-3'

domain. This mutation was similarly performed in both AADA-eGFP and TMD-eGFP constructs. Wild type and both mutant TMD-eGFP constructs were amplified by PCR using the following conditions: 95 °C for 2 min, 95 °C for 30 seconds, 53 °C for 20 seconds, 72 °C for 25 seconds, repeat for 29 times, 72 °C for 10 min and 4 °C forever. Wild type and both mutant AADA-eGFP constructs were amplified by PCR using the following conditions: 95 °C for 4 min, 94 °C for 30 seconds, 56 °C for 30 seconds, 72 °C for 25 seconds, repeated second to fourth step for 34 times, 72 °C for 5 min and 4 °C forever. All PCR products and eGFP-N1 vectors were digested with the restriction enzymes *BglII* and *PstI*, then subsequently excised and ligated together by in-gel ligation in Low Melt Agarose (BioRad) at room temperature using T4 ligase (Invitrogen). All WT and mutant AADA-eGFP and TMD eGFP constructs were sequenced for fidelity and transfected into McArdle cells using Lipofectamine 2000 (Invitrogen) according to the descriptions in *Generation and cell culture of McArdle cell lines stably expressing FLAG-AADA cDNA*. Transfected cells were grown overnight on glass coverslips in DMEM containing 50 U/mL penicillin/streptomycin, 10 % horse serum and 10 % fetal bovine serum at 37 °C in humidified air containing 5 % CO_2. The resultant subcellular localization of the constructs was determined by confocal immunofluorescence techniques as described above.

Sodium carbonate extraction assay- McA cells transiently transfected with wild type or both mutant TMD-eGFP constructs were harvested in 1 mL of ice-cold homogenization buffer (10 mM Tris-HCl at pH 7.4, 250 mM sucrose, 5 mM EDTA and 1X complete protease inhibitor cocktail (Roche)) and sonicated for 20 seconds. The total

cell lysates were spun at 453 g for 3 min to remove cell debris. The supernatant was then subjected to centrifugation at 355,040 g for 45 min to separate the cytosol (supernatant) from the membranes (pellet). The pellets were resuspended in 0.2 M Na_2CO_3 solution, pH 12.0 and incubated on ice for 30 min to allow release of membrane luminal contents. The samples were spun again at 355,040 g for 45 min to separate membrane luminal contents (supernatant) from membranes (pellet). 50 μL of cytosolic, membrane luminal and membrane fractions were boiled in 1X SDS-PAGE loading buffer and resolved by 10 % SDS-PAGE gel. The remaining procedures were described in *Immunoblotting techniques* in this section.

RNA isolation and real-time quantitative PCR for quantification of AADA mRNA expression- Total RNA was isolated from AADA transfected McA cells as well as 4 fasted and 4 fed female wild type C57BL/6J mouse livers using Trizol® reagent. First strand cDNA synthesis from 2 μg of total RNA was performed using SuperScript™ II reverse transcriptase (Invitrogen) primed by oligo dT primers (Invitrogen). PCR was performed using the mouse AADA primers: 5'ATA TAC CGC TTC CAG ATG CTA TT'3 and 5'TAT ATG CGG ACG GGA ACA CT'3. Primers for cyclophilin were: 5'TCC AAA GAC AGC AGA AAC TTT CG3' and 5' TCT TCT TGC TGG TCT TGC CAT TCC3'. PCR amplification of AADA cDNA was performed using the following conditions: 95 °C for 4 min, 94 °C for 30 seconds, 56 °C for 30 seconds, 72 °C for 20 seconds, repeated second to fourth step for 34 times, 72 °C for 5 min and 4 °C forever. The cDNA from one of the fed mouse livers was diluted 1/10, 1/40, 1/160, 1/640 and 1/2560 fold for preparation of a standard curve. All 8 cDNA samples were diluted 1/100

41

fold. Quantitation of AADA cDNA was performed using Platinum® SYBR®Green qPCR SuperMix-UDG (Invitrogen) by Rotor-Gene 3000 with Rotor-Gene 6.0 software.

Statistical analysis- Comparisons between 3 groups (control and 2 AADA-expressing cell lines) were analyzed by two-way ANOVA test using the software GraphPad PRISM® 4. All values are presented as means ±SD. Statistically significant differences were defined as those with values of *$p<$ 0.05 and **$p<0.01$ and ***$p<0.001$.

CHAPTER 3

SUBCELLULAR LOCALIZATION AND

MEMBRANE RETENTION MECHANISM OF MOUSE

AADA

3-1 Generation of polyclonal antibodies against mouse AADA

Polyclonal antibodies against mouse AADA were generated and the titre of the anti-AADA sera was determined by dot blot assay as described in Chapter 2. As shown in Figure 3-1, a 1:1000 dilution of the sera collected after the second and third booster injections of the conjugated-AADA peptide provides a good immunoreactive signal that is absent in the pre-immune sera at the same dilution. Therefore, all subsequent western blots requiring detection of AADA using this polyclonal antibody were performed at a dilution of 1:1000.

McA cells stably transfected with an empty pCI-neo vector or the same vector encoding mouse AADA cDNA with a FLAG tag engineered in just prior to the stop codon were generated as described in Chapter 2. Two different AADA-expressing clones (A13 and A23) were used in experiments presented in this Thesis. Immunoblots of total cell membrane fractions prepared from A13 and A23 cell lines with anti-AADA sera (Figure 3-2A) revealed an immunoreactive band of expected molecular mass (50 kDa) that was not present in total cell membrane fractions isolated from the empty vector transfected McA cells. On the other hand, the levels of calnexin, a loading control, was equal in both control and AADA expressing cell lines, indicating that stable McA cell lines expressing AADA have been generated successfully. Data presented in Figure 3-2A show that AADA protein levels in transfected McA cells are lower than in mouse liver. This weaker immunoreactive signal is not likely due to binding interference from the FLAG epitope at the C terminus but lower protein expression because measurement of mRNA expression by real time PCR revealed that McA cells transfected with AADA

1/33 1/100   1/330   1/1K   1/3.3K 1/10K 1/33K 1/100K 1/330K

Pre-immune

2nd boost

3rd boost

Figure 3-1. **Determination of the titre of anti-AADA sera.** Serial dilutions of pre-immune and anti-AADA sera were prepared at 1/33, 1/100, 1/330, 1/1000, 1/3300, 1/10,000, 1/33,000, 1/100,000, 1/330,000 with 3 % BSA/PBS. A nitrocellulose membrane was pre-incubated with 5 μg/mL of BSA-peptide in PBS and then blocked with 3 % BSA in PBS as described in Chapter 2. 1 μL of each diluted sera was spotted onto nitrocellulose membrane. The membrane was incubated at room temperature for 30 min and then incubated with goat anti-rabbit-HRP at 1:10,000 dilution in 1 % BSA for 1 hour. Immunoreactivity was detected by addition of ECL reagents followed by exposure to Biomax MR films.

45

A

pNeo   A13   A23   MLM   MBH

52 kDa —   — AADA

37 kDa —

93 kDa —   ← Calnexin

B

mRNA, ADA : Cyclophilin (Arbitrary Units)

1
0.9
0.8
0.7
0.6
0.5
0.4
0.3
0.2
0.1
0

Mouse Liver   pNeo   A13   A23

Figure 3-2. **AADA levels in mouse liver microsomes and transfected McA cells.** (A), Twenty µg of total cellular membrane proteins from stably transfected McA cells and from mouse liver microsomes (MLM) were electrophoresed, transferred to a nitrocellulose membrane and immunobloted with anti-AADA and anti-calnexin antibodies as described in *Immunoblotting techniques* in Chapter 2. AADA is not expressed in mouse brain and mouse brain homogenate (MBH) was used as a negative control. Calnexin was used as a loading control. (B), Two µg of total RNA was extracted from a wild type C57BL/6J mouse liver, A13 and A23 cell lines using Trizol® reagent. Total RNA was reverse transcribed to total cDNA and AADA cDNA was amplified by PCR according to conditions described in *RNA isolation and real-time quantitative PCR for quantification of AADA mRNA* in Chapter 2. Quantification of AADA cDNA was performed using Platinum® SYBR® Green qPCR SuperMix-UDG (Invitrogen) by Rotor-Gene 3000 with Rotor-Gene 6.0 software. This figure shows the AADA mRNA expression levels in mouse liver and the AADA cell lines relative to the housekeeping gene cyclophilin.

cDNA had lower AADA mRNA expression compared to mouse liver (Figure 3-2B). As Figure 3-2B shows, there is almost undetectable levels of AADA mRNA in the control cell line, whereas A13 and A23 cell lines have similar levels of AADA mRNA. The similarity in AADA mRNA expressions in the two cell lines strongly reflects the similarity in protein expressions. Although there has not been success in establishing a McA cell line with higher AADA expression, the functional studies discussed in Chapter 4 suggest that even relatively low AADA expression levels can result in alterations in hepatic lipid metabolism in McA cells.

3-2   Subcellular localization of mouse AADA

Previous work with carbonate extraction assays performed by a former graduate student in the laboratory demonstrated that AADA is a membrane protein. While alkaline carbonate was able to release luminal contents from isolated microsomes, AADA remained associated with the pelleted membrane fraction. To determine the precise subcellular location of AADA, immunocytochemistry was performed using mouse hepatocytes as described in Chapter 2. The rationale for using mouse hepatocytes as opposed to AADA-transfected McA cells is the high degree of specificity of anti-AADA antibody in mouse liver microsomes, and also in total liver homogenates, but not in the transfected cells (Figure 3-2A). Indeed, when anti-AADA antibody was used to detect AADA in transfected McA cells by immunocytochemistry, a signal was also present in the pNeo control cells (Figure 3-3A), suggesting that the staining pattern did not represent that of AADA. In mouse hepatocytes, the resultant localization of AADA

A

B
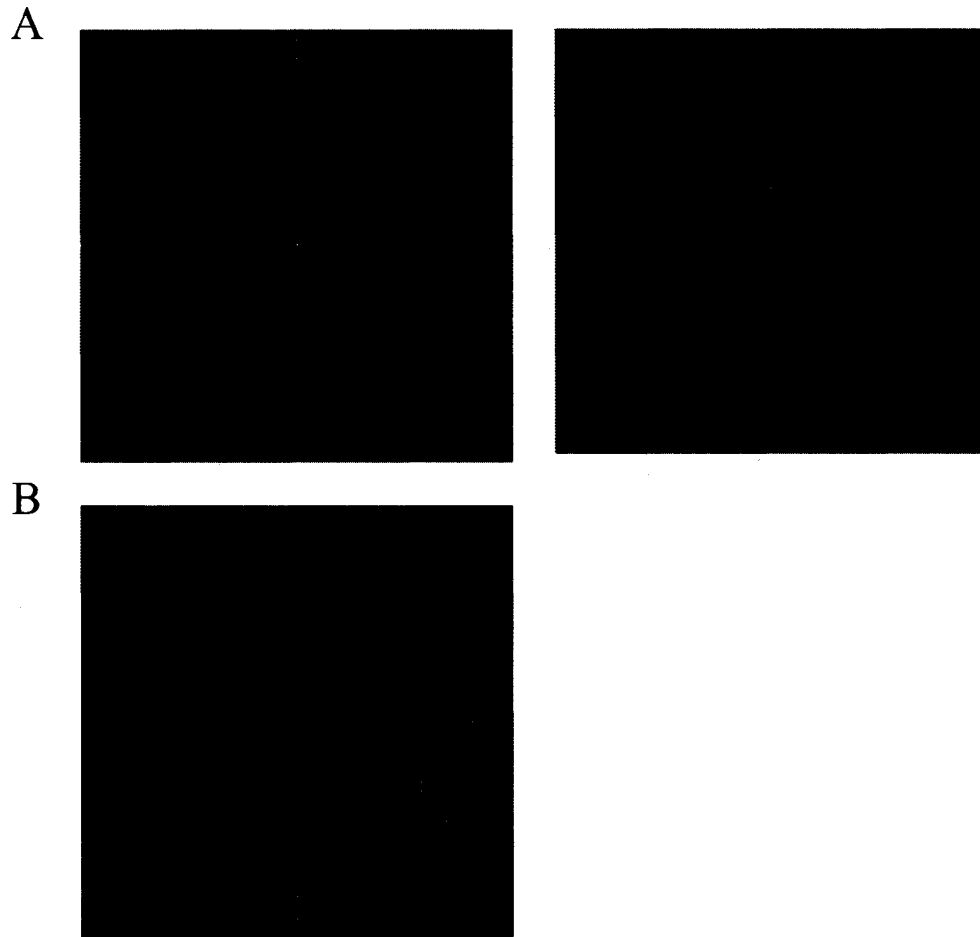
Figure 3-3. **AADA is localized to the ER in mouse hepatocytes.** (A), McA cells transfected with the empty vector pCIneo (left panel) and AADA (right panel) were grown on coverslips in conditions described in *Confocal immunofluorescence imaging of McArdle cells* in Chapter 2. Cells were fixed, incubated with primary rabbit anti-AADA and mouse anti-PDI antibodies, followed by incubation with secondary goat anti-rabbit Alexa 488 and donkey anti-mouse Texas Red antibodies. Green (lower left) = non-specific signal; Red (upper left) = ER maker, protein disulfide isomerase (PDI); Yellow (lower right) = image overlap; Black (upper right) = phase contrast setting turned off   (B), Mouse hepatocytes were grown on collagen coated coverslips in conditions described in *Confocal immunofluorescence imaging of mouse hepatocytes* in Chapter 2. Cells were fixed, incubated with primary rabbit anti-AADA and mouse anti-PDI antibodies, followed by incubation with secondary goat anti-rabbit Alexa 488 and donkey anti-mouse Texas Red antibodies. Green (lower left) = AADA; Red (upper left) = ER marker, PDI; Yellow (lower right) = image overlap; Black (upper right) = phase contrast setting turned off. All coverslips were mounted on glass slides with Prolong®Antifade Kit mounting medium and visualized by confocal immunofluorescence microscopy.

revealed a pattern that was typical of ER, which could be seen by the extent of co-localization with calnexin, an ER marker (Figure 3-3B). This staining pattern likely corresponds to AADA since its antibody can specifically recognize it on western blot. Additional evidence was also obtained from subcellular fractionation studies, where an aliquot of mouse liver homogenate was separated into fractions by ultracentrifugation in a Nycodenz gradient as described in Chapter 2. Immunoblots of isolated fractions concentrated by acetone precipitation showed enrichment of AADA in the ER fractions, but not in the Golgi fractions (Figure 3-4). From both studies, it can clearly be demonstrated that AADA is an ER-localized protein. Since the enzymes of the glycerol-3-phosphate pathway of glycerolipid synthesis are localized to the ER, it is reasonable for an enzyme with a proposed role in hepatic lipid metabolism to be localized in the same subcellular compartment.

3-3   Membrane topology of mouse AADA

A glycosylation assay was performed to assist with the determination of AADA topology. Since mouse AADA contains one potential N-glycosylation site in its C terminal domain, it is hypothesized that if this site is glycosylated, the C terminal domain must face the lumen of the ER where the addition of carbohydrate moieties to proteins takes place. Total cell lysates prepared from AADA transfected McA cells were treated with two glycosidases: Endo H and PNGase F. PNGase is a non-specific glycosidase that cleaves almost all N-linked oligosaccharides, and Endo H is a glycosidase that specifically cleaves high-mannose oligosaccharides.

1 2   3   4   5   6   7   8   9   10 11 12 13 14 15

— Calnexin

— TGN
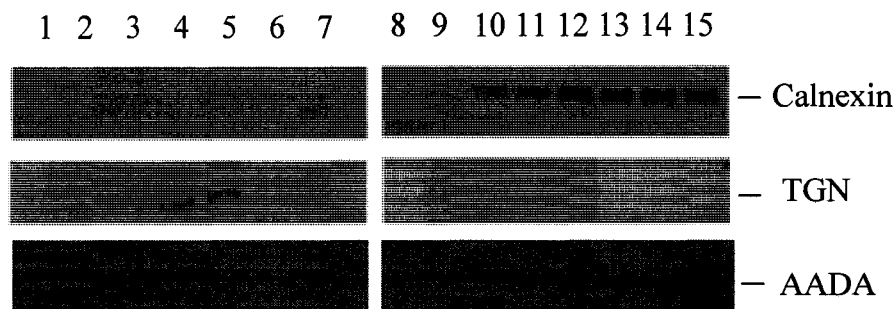
— AADA

Figure 3-4. **Subcellular fractionation studies confirm the ER localization of AADA.** 1 mL of mouse liver homogenate from wild type C57 BL/6J mouse was subjected to centrifugation at 10,000 g for 10 min to obtain post-nuclear supernatant. The supernatant was separated into subcellular fractions by ultracentrifugation at 169,044 g for 1.5 hours in a Nycodenz gradient. Fifteen 800 µL fractions were isolated and a 160 µL aliquot was subjected to acetone precipitation. The acetone precipitated pellets were resuspended in 50 µL of 1X SDS-PAGE loading buffer and separated by 10 % SDS-PAGE. Proteins were transferred to nitrocellulose membrane and incubated with anti-AADA, anti-calnexin and anti-TGN primary antibodies followed by incubation with secondary antibodies conjugated to HRP as described in *Immunoblotting techniques* in Chapter 2. Fraction 1 represents the top fraction with the lowest density, and the following fractions are loaded in order of increasing density, with fraction 15 being the last fraction isolated from the gradient.
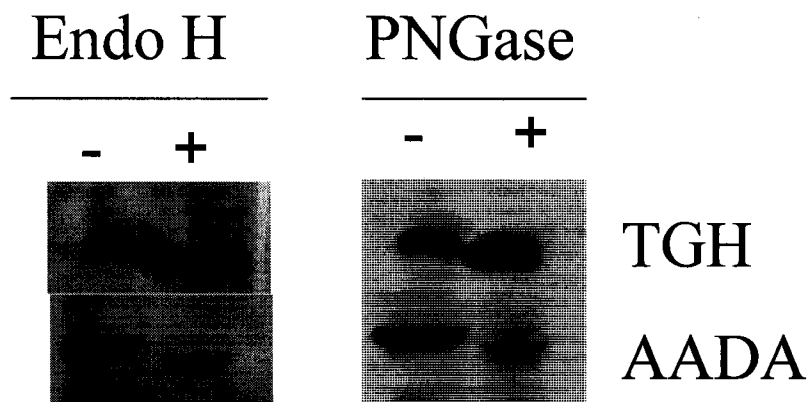
Figure 3-5. **AADA is an N-linked glycosylated ER transmembrane protein with type II conformation.** Cell lysates from A13 and TGH McA cell lines were treated with PNGase F and Endo H as described in *Glycosidase F (PNGase F) treatment* and *Endoglycosidase H (Endo H) treatment* in Chapter 2. Samples were boiled for 5 min in 1X SDS-PAGE loading buffer and resolved by 10 % SDS-PAGE. TGH was used as a positive control. AADA and TGH were visualized by immunoblotting with anti-FLAG antibodies and anti-TGH sera.

In both treatments, AADA and TGH (positive control) exhibited faster migration in SDS-PAGE gel, indicating that the protein is an N-linked glycoprotein with high mannose content (Figure 3-5). From this experiment, the orientation of AADA across the

ER membrane was also revealed. Based on the fact that the glycosylation site of AADA is located at the C-terminal domain of the protein, it can be deduced that AADA possesses a type-II conformation with the N-terminal portion facing the cytosol, and the C-terminal portion facing the ER lumen. Besides the subcellular localization of a protein, the membrane orientation may also be crucial to its function. In the case of AADA, its membrane orientation may determine its function as well as the fate of its hydrolysis products.

3-4   Membrane retention mechanism of mouse AADA

A di-arginine sequence located at the cytosol-oriented N-terminus was proposed to be essential for ER localization of type II transmembrane proteins (Ozols, 1998). AADA is a type II ER transmembrane protein, but lacks the di-arginine sequence at its N-terminus (Ozols, 1998). Therefore, it remains unclear how AADA is retained in the ER. To date, there are two type II ER resident proteins that have no obvious retention signals: 11β-hydroxysteroid dehydrogenase and AADA. While the retention mechanisms of these ER resident type II proteins are still unknown, there are models proposed to explain the mechanisms of Golgi retention of type II Golgi transmembrane proteins. One model suggests that retention depends on the length of the membrane spanning domain, which is reflected by the specific lipid composition of the Golgi membrane (Mziaut, 1999). The second model postulates that retention is achieved through oligomerization, which in turn

prevents proteins from exiting this subcellular compartment (Mziaut, 1999). From these studies, I hypothesized that similar mechanisms such as properties of the transmembrane domain of AADA and self-aggregation can be utilized by AADA for ER retention.

In order to study the potential retention properties in the transmembrane domain of AADA, two sets of mutations were introduced by site-directed mutagenesis to determine if any of these changes would alter ER retention properties of AADA. First of all, an eGFP-tagged AADA construct was generated and images obtained by confocal immunofluoresence microscopy confirmed that AADA-eGFP has the same subcellular localization as the native protein (Figure 3-6). In the first set of mutations, the transmembrane domain length was increased by the addition of 8 hydrophobic amino acids, resulting in a transmembrane domain with 25 amino acids, a length that is normally sufficient for insertion into the cholesterol-rich plasma membrane (Figure 3-7A). Results from immunocytochemistry studies indicated that increasing the length of the transmembrane domain did not alter the localization of the VL-AADA-eGPFP construct (Figure 3-7B), but when the same mutation was introduced in the eGFP-tagged transmembrane domain (TMD) fragment of AADA (consists of the first 29 amino acids from the N-terminus), the construct was partially re-directed to the Golgi (Figure 3-7C). These findings suggest that increasing the length of the transmembrane domain is not sufficient for the export of AADA from the ER and other signals exist within AADA for ER localization. In the second set of mutations, the three tyrosine residues in the evolutionarily conserved tyrosine-rich cluster within the predicted transmembrane domain were mutated to phenylalanines (Figure 3-8A). These evolutionarily conserved polar residues are not normally present in the transmembrane domain of membrane
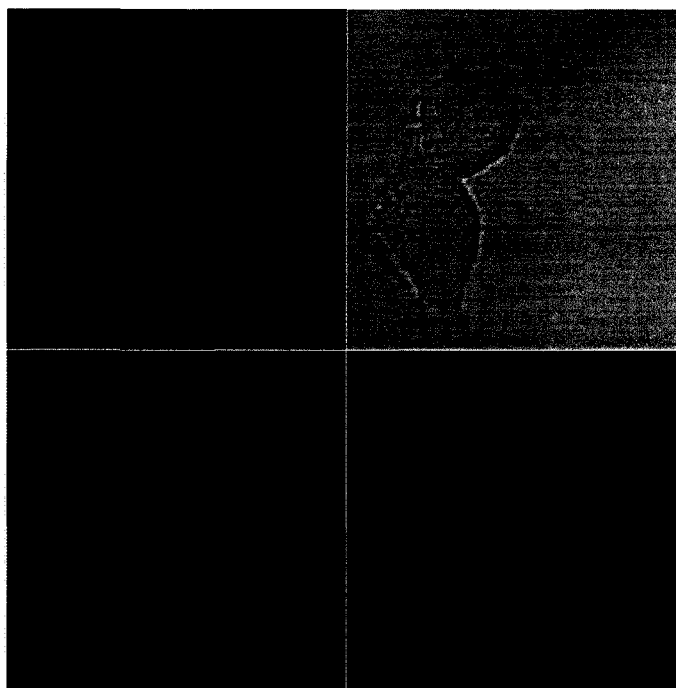
Figure 3-6. **Introduction of eGFP tag does not alter the ER localization of AADA.** The cDNA of mouse AADA was cloned into pEGFP-N1 vector using the restriction enzymes *BlgII* and *PstI*. McA cells transiently transfected with AADA-eGFP were grown on glass coverslips overnight, fixed with 4 % paraformaldehyde and permeabilized with 0.2 % Triton X-100 as described in *Confocal immunofluorescence imaging of McArdle cells*. The coverslips were incubated with primary mouse anti-eGFP and rabbit anti-calnexin antibodies, and then incubated with secondary goat-anti-mouse Alexa 488 and donkey anti-rabbit Texas Red antibodies. The coverslips were mounted on glass slides with Prolong®Antifade Kit mounting medium and visualized by Confocal Immunofluorescence Microscopy. Green (lower left) = AADA-eGFP; Red (upper left) = ER marker, calnexin; Yellow (lower right) = overlap; Black (upper right) = phase contrast.

FIGURE 3-7. **Increasing transmembrane domain length by 8 amino acids does not alter ER localization of VL-AADA-eGFP but redirects VL-TMD-eGFP to the Golgi.** (A), A schematic showing the location of the additional 8 alternating valine/leucine residues within the transmembrane domain. The cDNA of VL-AADA (B) and VL-TMD (C) were cloned into pEGFP-N1 vector using the restriction enzymes *BlgII* and *PstI.* McA cells transiently transfected with the eGFP constructs were grown on glass coverslips overnight, fixed with 4 % paraformaldehyde and permeabilized with 0.2 % Triton X-100 as described in *Confocal immunofluorescence imaging of McArdle cells.* The coverslips were incubated with primary mouse anti-eGFP and rabbit anti-Calnexin antibodies or rabbit anti-Mannosidase II antibodies, and then incubated with secondary goat-anti-mouse Alexa 488 and donkey anti-rabbit Texas Red antibodies. The coverslips were mounted on glass slides with Prolong®Antifade Kit mounting medium and visualized by Confocal Immunofluorescence Microscopy. Green = VL-AADA-eGFP (B) or VL-TMD-eGFP (C); Red = ER marker, calnexin (B) or Golgi marker, mannosidase II (C); Yellow = image overlap; Bright field = phase contrast.

A

ISLLISVVLVA<u>YYLYIP</u> ➡ **ISLLISVVVLVLVLVLLVA<u>YYLYIP</u>**

B

Calnexin

VL-AADA
eGFP
Overlap
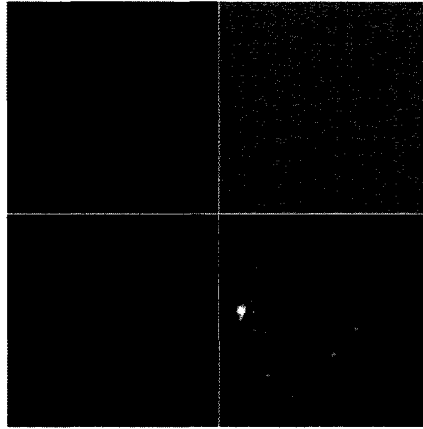
C

Mannosidase II
VL-TMD-eGFP

Overlap
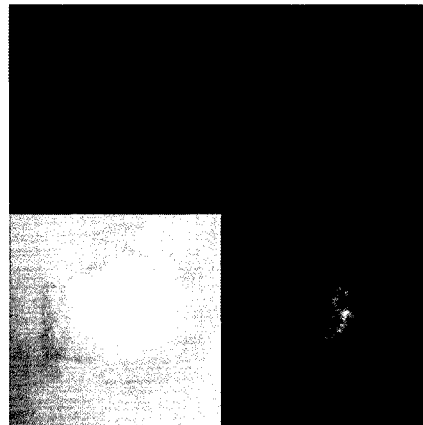
Figure 3-8. **Mutating the tyrosine residues to phenylalanines in the transmembrane domain does not alter ER localization of YF-AADA-eGFP but redirects YF-TMD-eGFP to the Golgi.** (A), A schematic showing the locations of the 3 tyrosine residues that were mutated to phenylalanines within the transmembrane domain. The cDNA of YF-AADA (B) and YF-TMD (C) were cloned into pEGFP-N1 vector using the restriction enzymes *BlgII* and *PstI*. McA cells transiently transfected with the eGFP constructs were grown on glass coverslips overnight, fixed with 4 % paraformaldehyde and permeabilized with 0.2 % Triton X-100 as described in *Confocal immunofluorescence imaging of McArdle cells*. The coverslips were incubated with primary mouse anti-eGFP and rabbit anti-Calnexin antibodies or rabbit anti-Mannosidase II antibodies, and then incubated with secondary goat-anti-mouse Alexa 488 and donkey anti-rabbit Texas Red antibodies. The coverslips were mounted on glass slides with Prolong®Antifade Kit mounting medium and visualized by Confocal Immunofluorescence Microscopy. Green = YF-AADA-eGFP (B) or YF-TMD-eGFP (C); Red = ER marker, calnexin (B) or Golgi marker, mannosidase II (C); Yellow = image overlap; Bright field = phase contrast.

A ISLLISVVLVA<u>YYLYIP</u> ⟶ ISLLISVVLVA<u>FFLFI</u>

[Tyr]   [Phe]
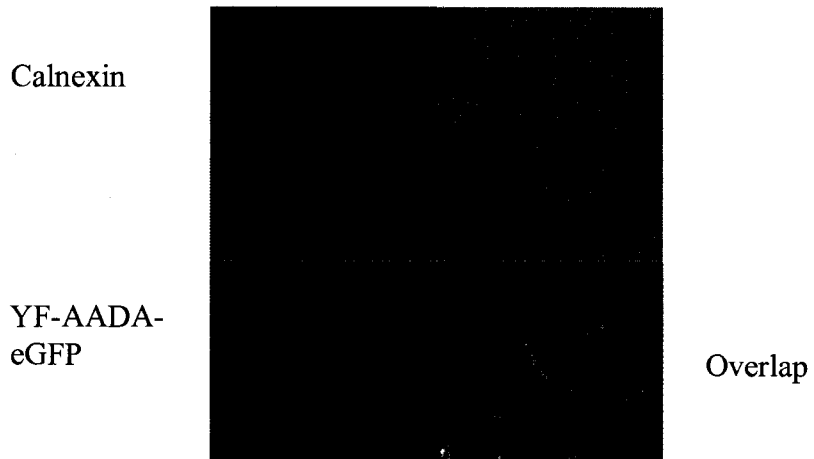
B

Calnexin

YF-AADA-
eGFP

Overlap

C

Mannosidase II

Overlap

YF-TMD-eGFP

58
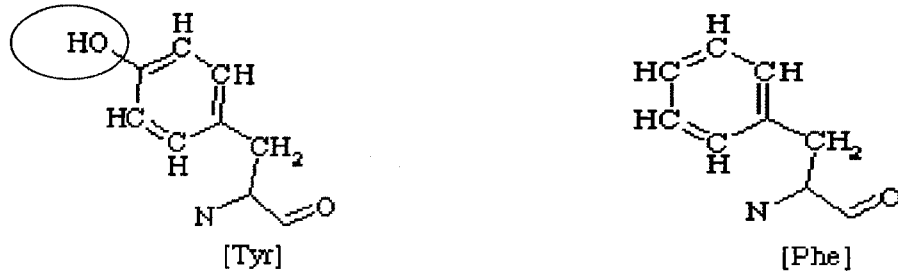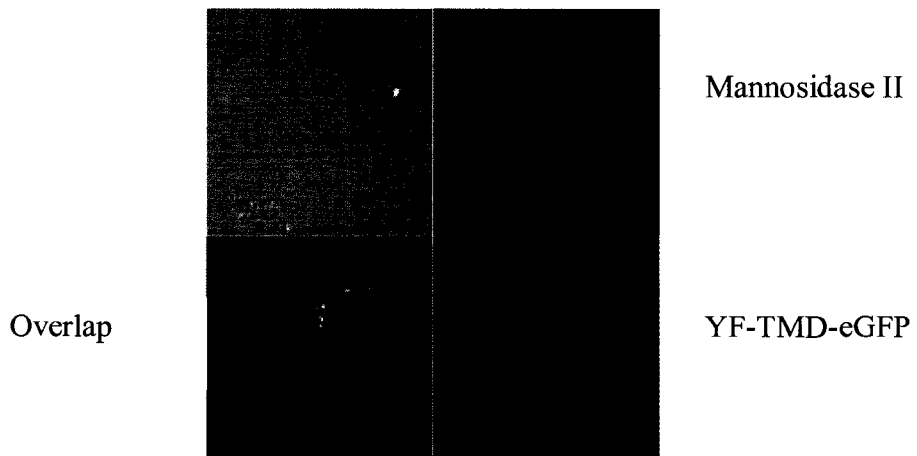
proteins, and by mutating these residues to structurally similar but non-polar phenylalanines, it can be shown whether polarity is responsible for ER retention. Immunocytochemistry studies showed that such mutation in the full length AADA did not alter the localization of the construct (Figure 3-8B), but the same mutation in the TMD-eGFP construct resulted in partial re-localization to the Golgi (Figure 3-8C). These results again show that the transmembrane domain contains properties that are critical for ER retention since only the wild-type TMD-eGFP (Figure 3-9A), but not the two mutants tested, was localized to the ER. In addition, when eGFP was expressed alone, the protein was distributed throughout the entire cell, indicating that the TMD fragment alone can direct the construct to the ER (Figure 3-9B). Since the confocal immunofluorescence images could not distinguish between membrane and luminal proteins, carbonate extraction assays followed by immunoblots of the eGFP constructs were performed as described in Chapter 2. An immunoblot of total cell lysates of McA cells transfected with either wild type or one of the two mutant TMD-eGFP constructs was able to confirm that all 3 constructs are membrane proteins (Figure 3-10). This suggests that the mutations did not alter the ability of the membrane spanning domain to insert into membranes, and all constructs appeared in the membrane fractions (Figure 3-10). Due to difficulties in improving transfection efficiency of AADA-eGFP and mutant AADA-eGFP constructs into McA cells, a similar experiment with these constructs was not possible. Since the mutations in the transmembrane domain did not alter ER localization of full length AADA, it is postulated that other yet to be identified mechanism(s) exists to retain AADA in the ER.

A   Calnexin

TMD-eGFP   Overlap

B

Calnexin   eGFP

                                            Overlap
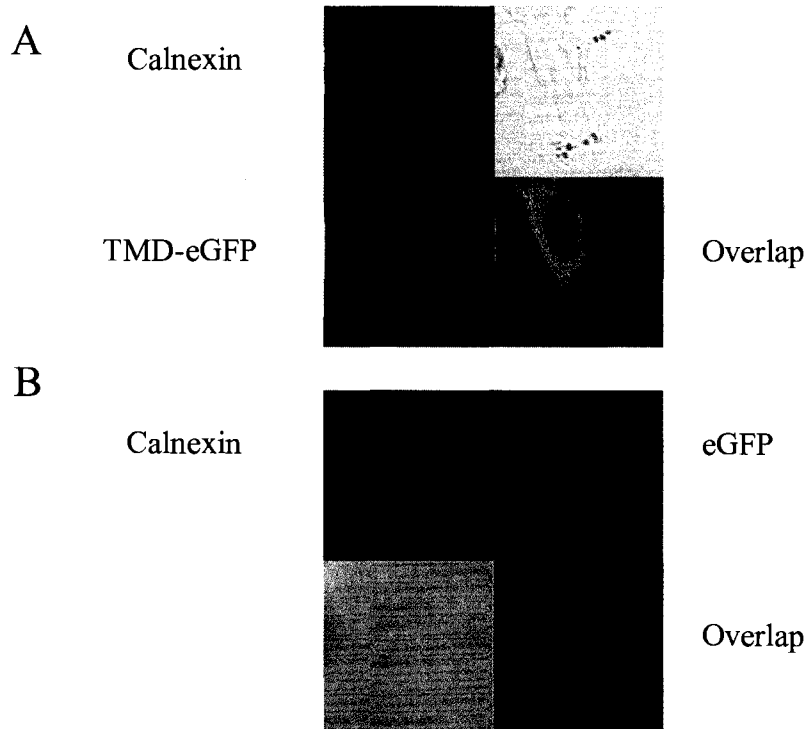
FIGURE 3-9. **The transmembrane domain fragment (TMD-eGFP) alone is sufficient for ER retention.** The cDNA of WT-TMD was cloned into pEGFP-N1 vector using the restriction enzymes *BlgII* and *PstI*. McA cells transiently transfected with the TMD-eGFP (A) or eGFP (B) constructs were grown on glass coverslips overnight, fixed with 4 % paraformaldehyde and permeabilized with 0.2 % Triton X-100 as described in *Confocal immunofluorescence imaging of McArdle cells*. The coverslips were incubated with primary mouse anti-eGFP and rabbit anti-Calnexin antibodies or rabbit anti-Mannosidase II antibodies, and then incubated with secondary goat-anti-mouse Alexa 488 and donkey anti-rabbit Texas Red antibodies. The coverslips were mounted on glass slides with Prolong®Antifade Kit mounting medium and visualized by Confocal Immunofluorescence Microscopy. Green = WT-TMD-eGFP (A) or eGFP (B); Red = ER marker, calnexin; Lower right = image overlap; Brightfield = phase contrast.

McA-WT-
TMD-eGFP

McA-YF-
TMD-eGFP

McA-VL-TMD-
eGFP

C L M   C L M   C L M

52 kDa —

37 kDa —

TMD-eGFP
constructs

McA-eGFP   McA

C L M   C L M

52 kDa —

37 kDa —
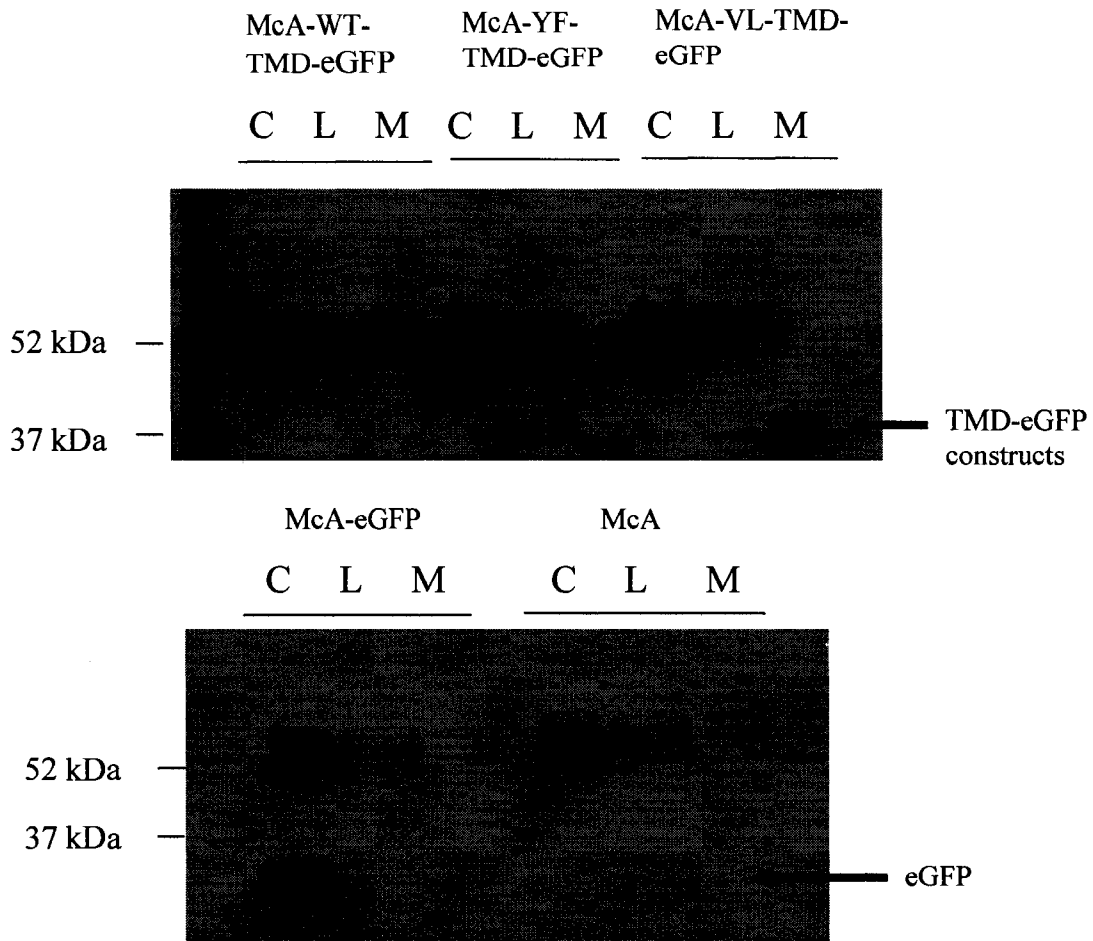
eGFP

Figure 3-10. **All wild type and mutant TMD-eGFP constructs remain as transmembrane proteins.** The cDNA of WT-TMD, YF-TMD or VL-TMD was cloned into pEGFP-N1 vector using the restriction enzymes *BlgII* and *PstI*. McA cells grown in 60 mm culture dishes were transiently transfected with the TMD-eGFP constructs. Cells were harvested in 1 mL of homogenization buffer and disrupted by sonication. The cells were spun at 453 g for 3 min to isolate cell debris. The supernantants were then subjected to ultracentrifugation at 355,040 g for 45 min to isolate membranes. The supernatants (cytosol) were kept and the pellets were resuspended in 1 mL of 0.2 M Na_2CO_3, pH 12.0. After brief sonication, the membrane samples were incubated for 30 min on ice and then centrifuged at 355,040 g for 45 min. The supernatants (luminal contents) were kept and the pellets (membranes) were resuspended in PBS. 50 μL of the cytosol (C), luminal contents (L) and membrane fractions (M) were subjected to 10 % SDS-PAGE followed by immunoblotting with primary mouse anti-eGFP antibodies and secondary goat anti-mouse HRP antibodies as described in *Sodium carbonate extraction assay* and *Immunoblotting techniques* in Chapter 2.

61

CHAPTER 4

ROLE OF MOUSE ARYLACETAMIDE DEACETYLASE IN

HEPATIC LIPID METABOLISM IN MCARDLE CELLS

4-1   Generation of McArdle cell lines stably expressing mouse AADA

The cell line chosen for these studies is a rat hepatoma cell line, McArdle RH7777 (McA), which are cells that are only capable of secreting newly synthesized TG and not TG from mobilized intracellular stores. Since McA cells do not express endogenous AADA, generation of stable McA cell lines expressing AADA would constitute a useful model to determine the functional role of AADA. Due to unavailability of antibodies specific against AADA at the start of the project, detection of protein expression was made feasible by engineering a FLAG epitope just prior to the stop codon of the cDNA of mouse AADA. The subsequent construct was stably transfected into McA cells. Two stable cell lines expressing FLAG-tagged mouse AADA were thereafter established and were denoted A13 and A23 (Chapter 3, Figure 3-2).

4-2   Effect of mouse AADA on lipid turnover and secretion

Prior to determining whether AADA has a role in hepatic lipid metabolism, AADA cell lines were first tested for *in vitro* esterase and lipase activities. To determine the presence of esterase activity, an activity-based probe, FP-biotin (Figure 4-1A) and a water-soluble esterase substrate, p- nitrophenyl acetate (p-NP acetate) (Figure 4-1B) were used. If AADA possessed esterase activity, its active site serine would undergo a nucleophilic attack on the phosphate group in FP-biotin, resulting in a covalent modification of the serine residue (Figure 4-1B). This biotinylated compound can then be detected by probing with streptavidin-HRP secondary antibodies as described in Chapter 2. The presence of esterase activity can also be detected by the release of a chromogenic

A

B

Reaction: E-Ser-OH + FP-O₃-biotin ⟶ E-Ser-O-P-O₃-biotin

C

D

Reaction: E-Ser-OH + Nitrophenyl-O-PO(OCH₂CH₃)₂ ⟶ E-Ser-O-PO(OCH₂CH₃)₂

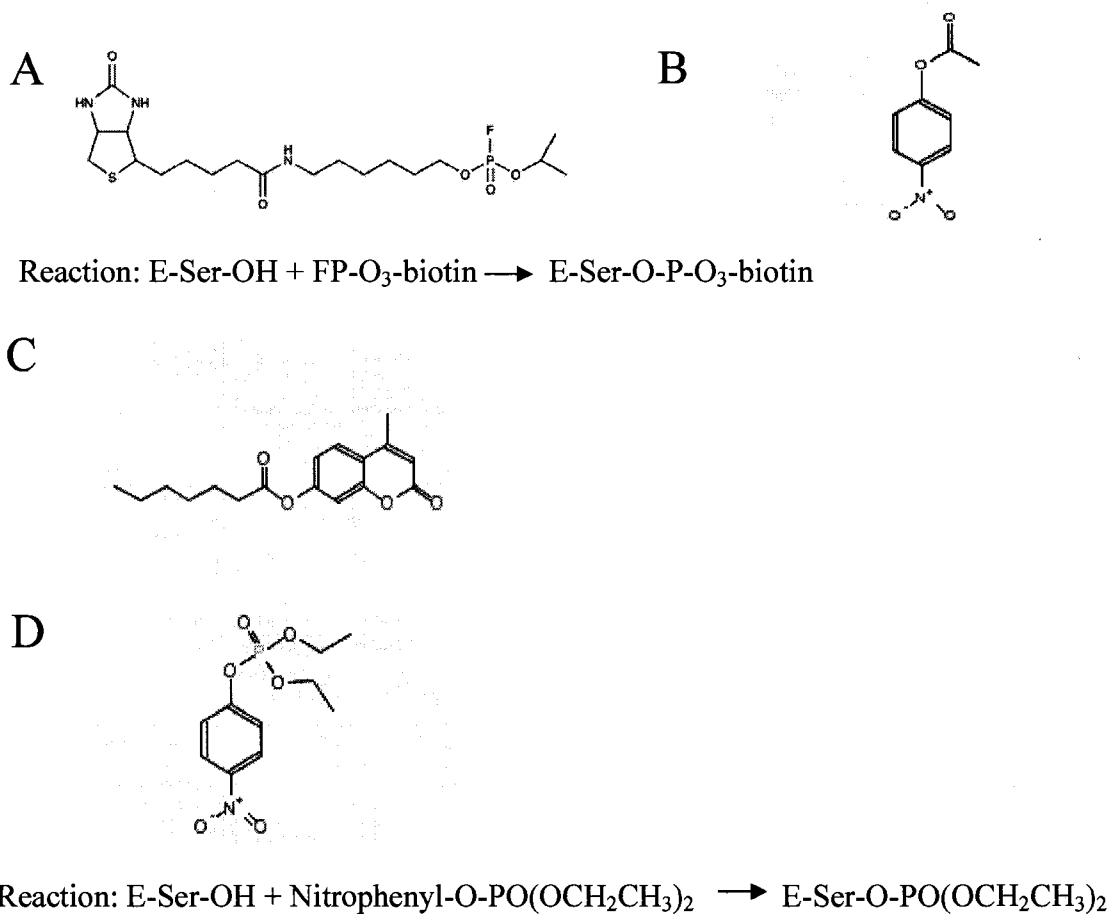Figure 4-1. **Molecular structure of inhibitors and substrates used for *in vitro* esterase and lipase activity assays and metabolic labeling studies.** (A), 6-N-Biotinylaminohexyl Isopropyl Phosphorofluoridate (FP-biotin) and mechanism of reaction. (B), *p*-nitrophenyl acetate (*p*-NP acetate). (C), 4-methylumbelliferyl-heptanoate (4-MUH). (D) Diethyl *p*-nitrophenyl phosphate (E600) and mechanism of reaction.

compound, *p*-nitrophenol (*p*-NP) from the water soluble substrate, *p*-NP acetate. The chromogenic compound *p*-NP absorbs at 405 nm, and therefore, an increase in absorbance at this wavelength would indicate accumulation of this product. Treatment with FP-biotin followed by probing with streptavidin-HRP revealed an immunoreactive band of expected molecular size of AADA (50 kDa) in the AADA transfected cell lysates, but not in the control cell lysates (Figure 4-2A). Moreover, *in vitro* activity assay against *p*NP-acetate suggested that AADA exhibited esterase activity that was absent in the control pNeo cell line (Figure 4-2B). These results are consistent with previous reports that AADA is an esterase (Probst *et al*, 1994) and suggest that AADA is also capable of hydrolyzing carboxylester bonds of lipid substrates.

To test for the presence of lipase activity in AADA, an artificial water-insoluble lipase substrate, 4-MUH was used. The existence of lipase activity would lead to hydrolysis of 4-MUH, releasing the fluorogenic compound, 4-MU. The extent of lipase activity is thus monitored by the amount of 4-MU formed in a measured period of time. Figure 4-2C shows that expression of AADA in McA cells results in a significant increase in activity against 4-MUH. This demonstrates that AADA possesses lipase activity against this artificial lipase substrate, which indicates AADA may act as a lipase in the liver.

Based on sequence homology with HSL and the results from *in vitro* activity assays, it is hypothesized that AADA is a lipase and has a role in hepatic lipid turnover. To test this hypothesis, McA pCIneo and AADA cells were incubated with 0.4 mM [^{3}H]OA for 4 hours. While some cells were collected for lipid analysis after the 4 hour pulse incubation with excess OA, some were rinsed briefly with DMEM and then

Figure 4-2. *In vitro* **esterase and lipase activity of AADA.** (A), 30 µg of total cellular proteins from McA pCI-neo, A13, A23 and WT-hTGH were treated with 1 % FP-biotin in 0.07 % Triton X-100 and incubated at room temperature for 30 min. Samples were resolved in 10 % SDS-PAGE, transferred to nitrocellulose membrane and immunoblotted with streptavidin-HRP. (B) and (C), 20 µg of total cellular membrane proteins prepared from McA cells stably transfected with an empty pCIneo vector, FLAG-tagged mouse AADA or human TGH in serum free DMEM were incubated with pNP-acetate (B) or 4-MUH (C). The release of pNP was monitored at 405 nm and that of 4-umbelliferone at 460 nm. The results are presented as an average from triplicate measurements.

A
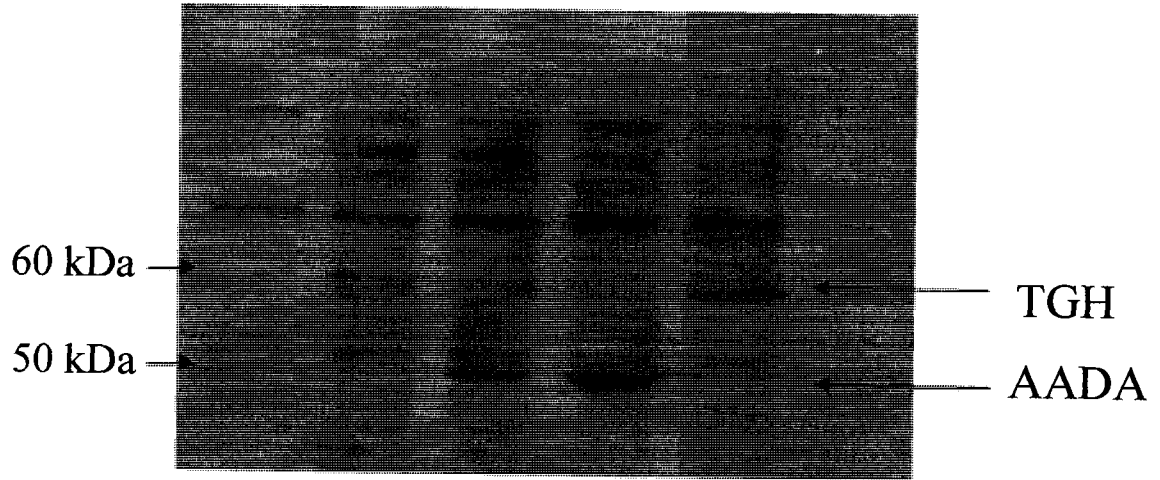
B
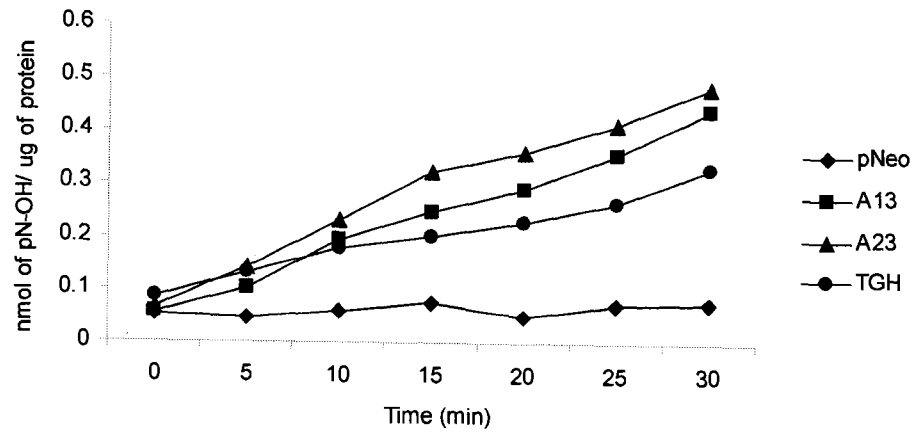
C
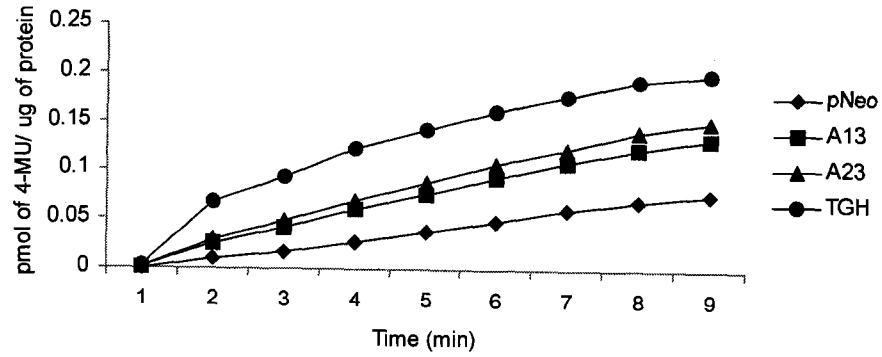
incubated with DMEM for an additional 4 hour chase, which was performed in the absence of excess OA. A detailed description of the procedures is included in Chapter 2.

After 4 hour pulse incubation with 0.4 mM [^{3}H]OA, both AADA expressing cell lines accumulated approximately 40 % less ($p<0.001$) intracellular TG than the control pCIneo cell line (Figure 4-3A). During the 4 hour chase, turnover of intracellular [^{3}H] TG was similar among all cell lines (Figure 4-3A). From these results, it can be speculated that AADA acts primarily on newly synthesized TG rather than preformed TG stores since intracellular TG decreased equally by 42 % in both control and AADA cell lines while this process occurred in the absence of excess OA in the medium. Interestingly, this reduction in intracellular TG was lost when the incubation mixture was supplemented with the lipase inhibitor E600 (Figure 4-3A). This suggests that active mobilization of TG in McA cells has been blocked effectively and the decrease in TG levels in AADA expressing cells was due to lipolytic activity of the enzyme rather than any possible effect(s) on fatty acid uptake and/or triacylglycerol synthetic enzymes. The specificity of the effect of AADA on lipolysis rather than synthesis was evident by similar levels of intracellular CE and phosphatidylcholine (PC) synthesis among all cell lines (Figures 4-3B and 4-3C, respectively). Similarly, inclusion of E600 during the chase incubations led to restoration of intracellular TG levels in AADA expressing cells to control level, indicating that turnover of preformed TG during the 4 hour chase period was also inhibited (Figure 4-3A).

To further confirm that TG levels are altered in AADA cell lines as a result of increased lipolysis and not decreased synthesis, TG synthesis was measured over a short 1 hour pulse labeling experiment. As shown in Figure 4-4A, intracellular [^{3}H] TG levels
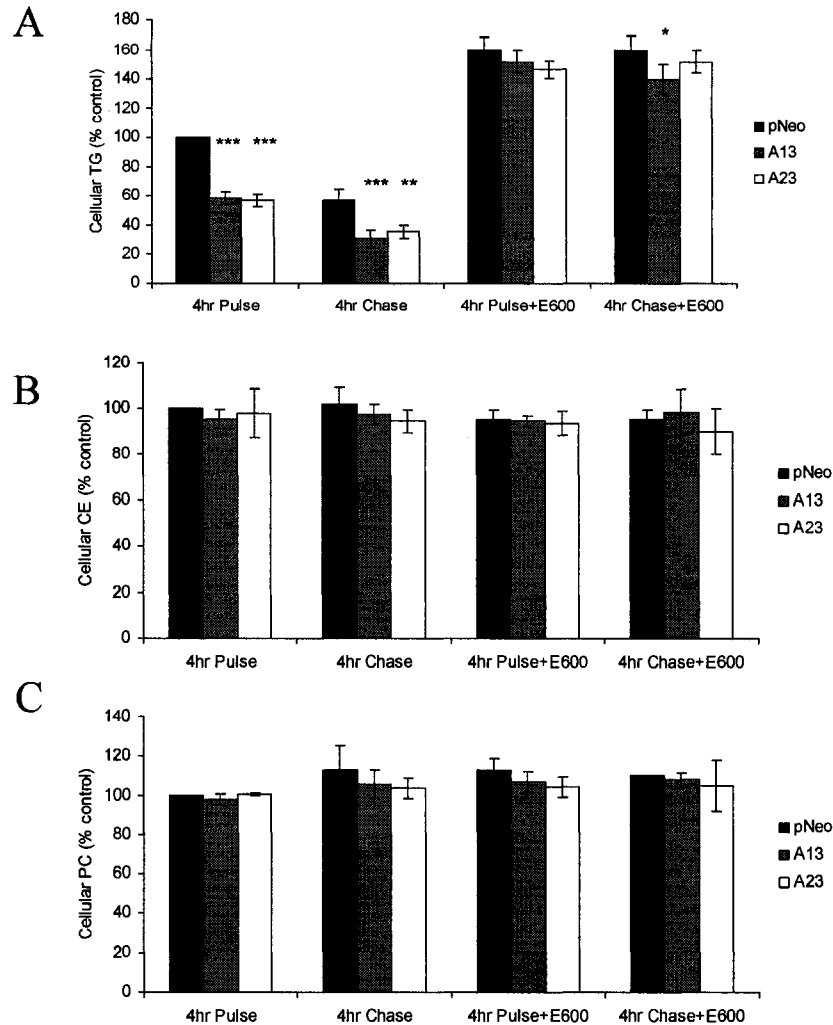
Figure 4-3. **AADA expression decreases levels of de novo synthesized [^{3}H] TG.** McA cells stably transfected with an empty pCIneo vector or pCIneo vector containing FLAG-tagged mouse AADA cDNA (A13 and A23) were incubated with 0.4 mM [^{3}H]OA in the presence or absence of a lipase inhibitor (E600) and harvested either after pulse or chase as indicated. Lipids were extracted and analyzed by thin-layer chromatography as described in *Metabolic labeling studies* in Chapter 2. The amount of radioactivity incorporated into TG (A), CE (B) and PC (C) was determined by scintillation counting. Due to slight variation in radioactivity incorporation in 3 independent experiments, the data presented are shown as percentages of the dpm counts per milligram of protein of control pCIneo at 4 hour pulse. The actual dpm/mg cell protein incorporated into cellular lipids for pCIneo at 4 hour pulse from 3 independent experiments performed in triplicates (mean±SD) were between 150,000±30,000 and 190,000±20,000 for TG, 50,000±9000 and 71,000±6300 for CE, and 100,000±5500 and 110,000±26,000 for PC. *$p<0.05$, **$p<0.01$ and ***$p<0.001$.

Figure 4-4. **AADA expression does not alter lipid synthesis.** McA cells stably transfected with an empty pCIneo vector or pCIneo vector containing FLAG-tagged mouse AADA cDNA (A13 and A23) were incubated with 0.4 mM [^{3}H]OA and harvested after the specified incubation times as described in Chapter 2. (A) and (B), Lipids were extracted and analyzed by thin-layer chromatography. The amount of radioactivity incorporated into TG (A) and PC (B) was determined by scintillation counting.

remained the same in all cell lines and a difference was not detected until after the first hour. In agreement with the data from long pulse labeling, PC synthesis remained the same in all cell lines up to the end of the time course (Figure 4-4B). In a separate 1 hour pulse labeling experiment, fatty acid uptake was also measured to be similar in both control and AADA McA cell lines (Figure 4-5).

In order to show that total lipid mass is also affected in a similar fashion, total lipid mass was analyzed by gas chromatography analysis. As data in Figure 4A shows, the reduction in TG labeling is indeed mirrored by the decrease in total TG mass in both AADA expressing cell lines after treatment with 0.4 mM OA for 4 hours. Moreover, addition of E600 abolished the difference in intracellular TG levels between AADA and control cell lines (Figure 4-6A). While a difference in intracellular TG accumulation between AADA expressing and control cells was observed, intracellular CE levels (Figure 4-6B) and intracellular PL levels (Figure 4-6C) remained relatively constant. These results further support the role of AADA in the regulation of cellular TG levels.

4-3   Effect of mouse AADA on apoB100 secretion from McA cells

Data in Figures 4-3 to 4-6 suggest that expression of AADA in McA cells reduces intracellular TG levels through increased TG hydrolysis. However, it is necessary to identify the consequences of AADA-mediated lipolysis in order to fully understand the role of AADA in lipid metabolism. Therefore, the first attempt was to determine whether the increase in lipolysis of intracellular TG by AADA would result in provision of substrates for secretion of apoB-containing particles. Densitometry analysis of
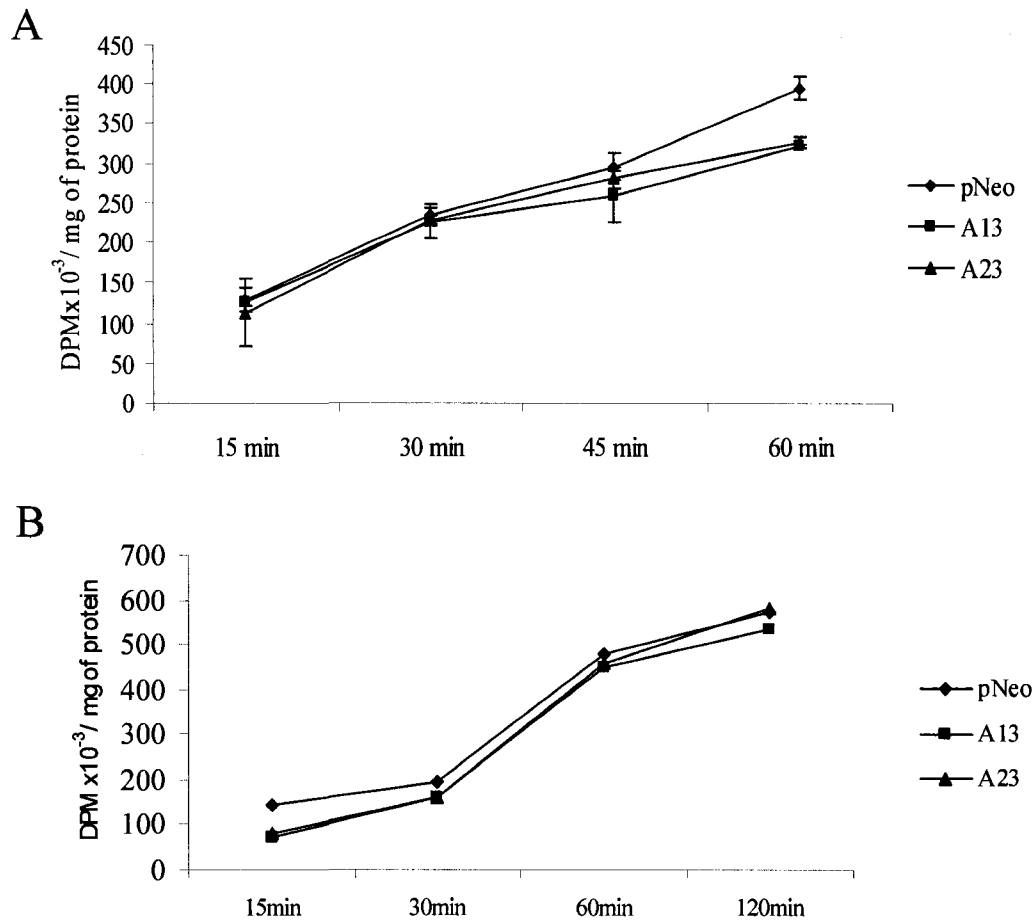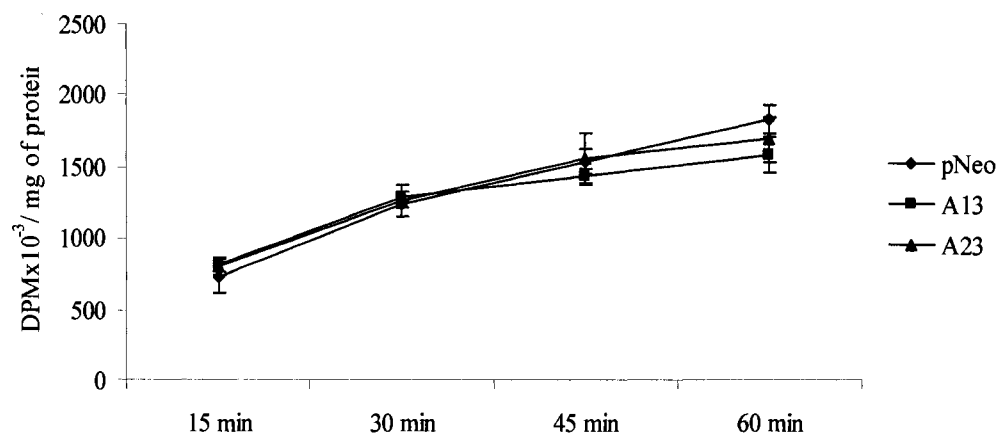
Figure 4-5. **AADA expression does not alter fatty acid uptake.** McA cells stably transfected with an empty pCIneo vector or pCIneo vector containing FLAG-tagged mouse AADA cDNA (A13 and A23) were incubated with 0.4 mM [^{3}H]OA and harvested after the specified incubation times as described in Chapter 2. An aliquot of the total cell lysates was measured for radioactive contents by scintillation counting.
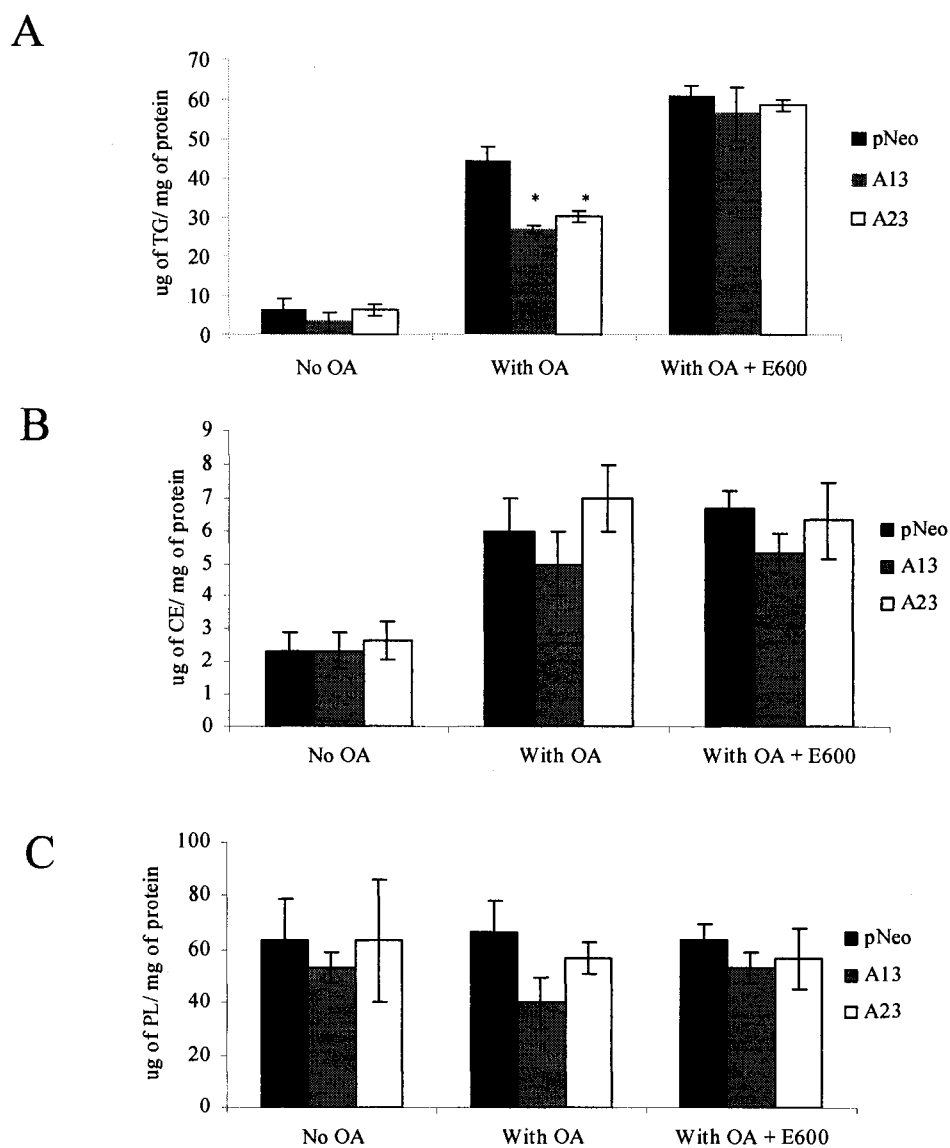
Figure 4-6. **AADA expression decreases cellular TG mass levels.** McA cells stably transfected with an empty pCIneo vector or pCIneo vector containing FLAG-tagged mouse AADA cDNA (A13 and A23) were incubated in serum-free DMEM in the presence or absence of 0.4 mM OA and in the presence or absence of a lipase inhibitor, E600, for 4 hours. Cells were harvested in 2 mL of ice-cold PBS, lipids were extracted and the mass of TG (A), CE (B) and phospholipids (PL) (C) was measured by gas chromatography as described in *Measurements of oleic acid incorporation into cellular lipids* in Chapter 2. The data presented are representative of 2 independent experiments. *$p<0.001$.

immunoblots of media apoB revealed that expression of AADA decreased apoB100 secretion in both cell lines while the secretion of albumin remained unaffected by AADA expression (Figures 4-7A and 4-7B). Although albumin secretion did not appear to be consistent among all three cell lines, there were difficulties in choosing an appropriate secretion control for Cab-O-Sil precipitation since this procedure may not ensure a uniform pull-down of non-hydrophobic proteins such as albumin. Analyses of media lipids from metabolic labeling studies showed that TG secretion was also lower in AADA expressing cells (Figure 4-7C). About 3.8 % of newly synthesized TG was secreted during the 4 hour OA incubations from control compared to 2.4 % from the A13 line and 2.7 % from the A23 line. This suggests that AADA cells not only secrete a decreased amount of TG, but also exhibit a lower rate of secretion of de novo synthesized TG. On the other hand, secretion of preformed TG during the chase period was similar in all cell lines, which represented about 0.7 % of cellular TG that had accumulated at the end of the pulse period (Figure 4-7C). A similar rate of TG secretion during the chase period is in agreement with the speculation that AADA acts mainly on newly made TG. In addition, the results suggest that increased hydrolysis of newly made TG in AADA cell lines does not lead to increased channelling of substrates for VLDL assembly. ApoB 100 secretion is reduced as a result of AADA expression in McA cells.

4-4   Effect of mouse AADA on fatty acid oxidation in McA cells

If expression of AADA increased lipolysis without increasing TG or apoB 100 secretion, another possible destination for the hydrolysed products is the mitochondria for β-oxidation. To measure fatty acid oxidation in cells, the amount of acid soluble
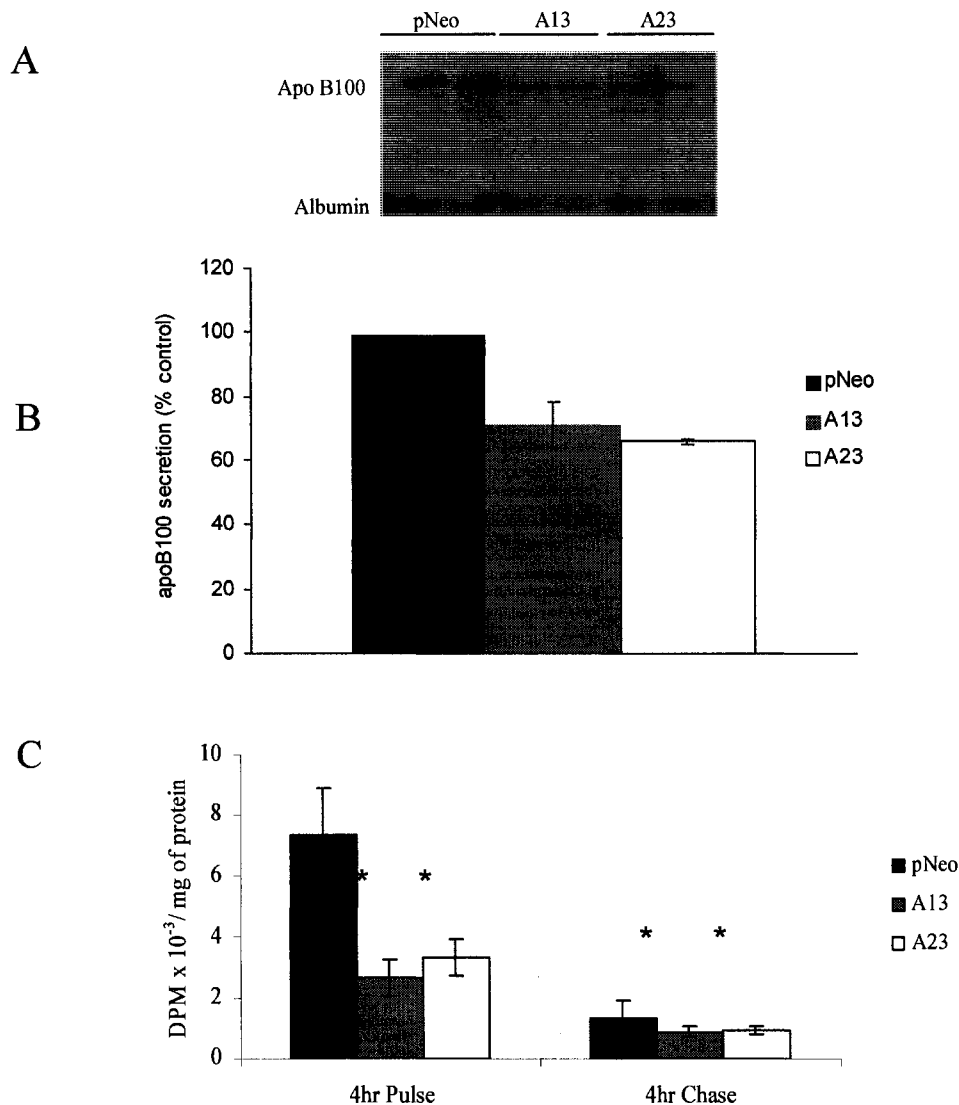
Figure 4-7. **AADA expression decreases apoB and TG secretion.** (A), Media from 100 mm dishes of McA cells stably transfected with an empty pCIneo vector or pCIneo vector containing FLAG-tagged mouse AADA cDNA (A13 and A23) were collected after 4 hour incubation with 0.4 mM OA. Media equivalent to 0.5 mg of cell protein were incubated with 50 mg/mL of Cab-O-Sil (fumed silica) at 4 °C for 45 min as described in *Secretion of apoB* in Chapter 2. Samples were electrophoresed in BioRad ready-gels, transferred to nitrocellulose membranes and immunoblotted with goat anti-apoB antibodies followed by rabbit anti-albumin antibodies also described in the same section of Chapter 2. (B), Densitometry analysis by Quantity One software (BioRad) on the amount of apoB100 secretion is expressed as a percentage of apoB100 secreted by the control cell line (pCIneo). (C), McA cells were incubated with 0.4 mM [^{3}H]OA for 4 hours. Cell media was subjected to lipid extraction and analysis. The amount of TG in media was measured by scintillation counting. The results in (A) and (B) are representative of 4 independent experiments. The results in (C) represent mean±SD from 3 independent experiments performed in triplicates. *$p < 0.001$.

metabolites (ASM) released into the media at the end of 4 hour pulse/chase experiments with 0.4 mM [^{3}H]OA was quantified. ASM are the by-products of β-oxidation, consisting mainly of acetyl-CoA and ketone bodies, which reflect the level of fatty acid oxidation in cells. The greater the amount of ASM detected in the media, the higher the rate of fatty acid oxidation. The level of ASM in media was augmented upon expression of AADA, which indicated an increase in fatty acid oxidation due to AADA expression (Figure 4-8). During the 4 hour chase period in the absence of exogenous fatty acids, the levels of fatty acids released from preformed stores for oxidation were similar among the cell lines, suggesting that AADA has a minor role in the mobilization of preformed TG stores for this process. Inclusion of E600 during the pulse incubations ablated the increase in β-oxidation in AADA cells, and the resultant oxidation levels were similar in both control and AADA cells. Thus, it appears that in the presence of exogenous fatty acids, at least 20 % of the fatty acids destined for β-oxidation is derived from hydrolysis of newly formed TG stores, and this mobilization can be blocked by lipase inhibitors. Since the delivery of exogenous fatty acids for β-oxidation in the presence of E600 is the same in control and AADA cells, this provides an additional evidence that fatty acid uptake by both control and AADA cells is similar, as seen in the cell labeling and lipid mass studies (Figures 4-3B and 4-6B, respectively).

4-5   Substrate specificity of mouse AADA

Despite of a better understanding of the downstream effects of AADA-mediated lipolysis, the substrate specificity of AADA is still unclear. For a more complete characterization of AADA function, the lipid profiles of cellular membranes
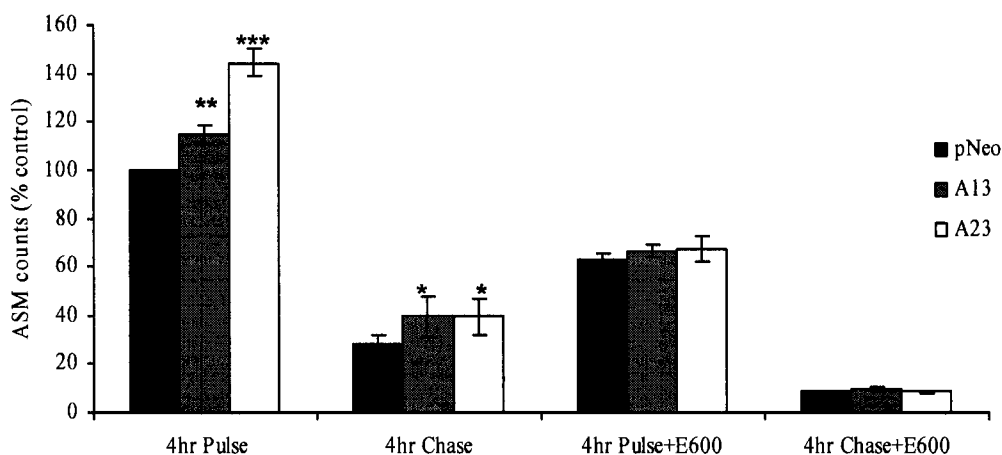
Figure 4-8. **AADA expression increases fatty acid oxidation.** McA cells stably transfected with an empty pCIneo vector and pCIneo vector containing FLAG-tagged mouse AADA cDNA (A13 and A23) were incubated with 0.4 mM [^{3}H]OA for 4 hours in the presence or absence of E600 (pulse), followed by incubation in DMEM with or without E600 (Chase). Media equivalent to 0.5 mg of cell protein was analyzed for radioactivity in acid-soluble metabolites (ASM) as described in *Fatty acid oxidation measurements* in Chapter 2. Due to variations in radioactivity incorporation in 3 independent experiments, the data presented are shown as percentages of control pCIneo at 4 hour pulse. The averages of the actual dpm/mg cell protein in ASM for pCIneo at 4 hour pulse from 3 independent experiments performed in triplicates (mean±SD) were between 610,000±70000 and 880,000±100,000. *$p<0.05$, **$p<0.01$ and ***$p<0.001$.

isolated from AADA transfected McA cells were studied over a time course. In addition, two natural lipid substrates, oleoyl-CoA and diacylglycerol (DG), have been tested for hydrolysis by AADA.

According to the metabolic labeling studies discussed in the previous section, expression of AADA in McA cells resulted in increased levels of fatty acid oxidation (Figure 4-8). It is therefore postulated that AADA may function as a lipase which hydrolyses lipid substrates to release free fatty acids that can be destined to the mitochondria for β-oxidation. In order to determine if AADA hydrolyzes specific lipid substrates to release fatty acids for β-oxidation, McA pCIneo and AADA cells were first incubated with 0.4 mM [^{3}H]OA, cellular membrane fractions were then isolated from control and AADA McA cells, and the fractions were incubated in the presence of 0.1 % BSA in PBS as described in Chapter 2. This experiment revealed a profile of endogenous lipids from each cell line, which was visualized by autoradiography as described in Chapter 2. While membranes isolated from both AADA expressing McA cell lines had accumulated fatty acids with time (Figures 4-9A and 4-9B), this was not seen in the control pNeo cell line (Figure 4-9C), suggesting that fatty acids were released as a result of AADA-mediated hydrolysis of lipid substrates. Accumulation of fatty acids was also observed in the Pancreatin containing fractions, and the source of these fatty acids was mainly attributed to PC hydrolysis (Figure 4-9D). On the other hand, there was no apparent disappearance of any lipid that could account for the increase in fatty acids in the AADA-McA membrane lipids (Figures 4-9A and 4-9B). Although this experiment is not able to identify any specific substrate(s) of AADA, it provides further support for its

A

Time (hours)

0   0   0   1   1   4   4

TG
FA

PC

B

Time (hours)

0   0   0   1   1   4   4

TG
FA

PC

C

Time (hours)

0   0   0   1   1   4   4

TG
FA

PC

D

Time (hours)

0   0   1   4

TG
FA

PC
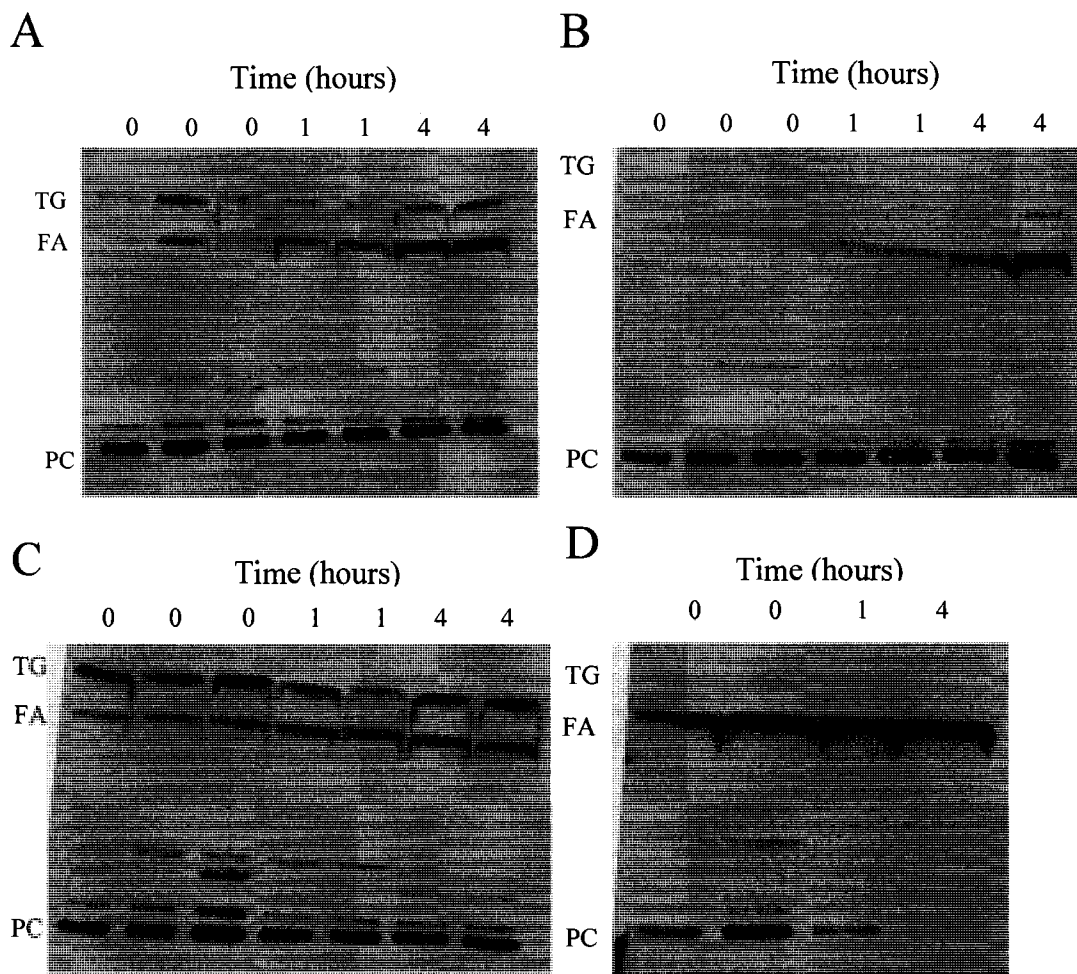
Figure 4-9. **AADA expression increases fatty acid accumulation in cellular membrane fractions.** McA cells stably transfected with an empty pCIneo vector or pCIneo vector containing FLAG-tagged mouse AADA cDNA (A13 and A23) were incubated with 0.4 mM [^{3}H]OA for 4 hours. Cellular membrane fractions prepared from A13 (A), A23 (B), pNeo (C) and pNeo with Pancreatin (D) were incubated with 0.1 % BSA/PBS for 0, 1 and 4 hours. The positive control (D) contains a mixture of McA-pNeo membranes and Pancreatin solution. Lipids were extracted at the end of the specified time points and separated by TLC as described in *Lipid profiles of microsomes derived from AADA-McA stable cell lines* in Chapter 2. Lipid profiles were visualized by autoradiography and densitometry analysis was performed using Quantity One software (BioRad) as described in Chapter 2.

proposed function in lipid metabolism by hydrolyzing lipid substrates and generating fatty acids that could be directed to the mitochondria, leading to increased rates of fatty acid oxidation (Figure 4-8).

In an *in vitro* hydrolase activity assay against the natural lipid substrate oleoyl-CoA, both pNeo control and AADA fractions exhibited similar levels of activity against the substrate, suggesting that AADA does not act specifically on oleoyl-CoA (Figure 4-10A). However, it is worth noting that the hydrolase activity detected in the McA membrane fractions is not significantly above background level. Therefore, the lack of activity against oleoyl-CoA may be due to requirements of specific assay conditions and it should not be excluded as an oleoyl-CoA hydrolase. Another natural lipid substrate tested was DG. AADA did not display lipolytic activity against this substrate (Figure 4-10B). Once again, AADA should not be excluded as a DG hydrolase based on results from this experiment since assay conditions may not be optimal for activity against this substrate.

Figure 4-10. **AADA exhibits weak hydrolytic activity against oleoyl-CoA and no hydrolytic activity against DG** *in vitro*. (A), 100 μM of oleoyl-CoA in 0.1 % CHAPS/PBS and 20,000 dpm of [^{14}C]oleoyl-CoA were mixed with 10 μg of total cellular membrane proteins derived from McA pCIneo and AADA cells in 0.1 % CHAPS/PBS. The reaction mixture was incubated for 30 min at 37 °C. The reaction was stopped by the addition of 4 mL of chloroform/methanol 2:1 containing lipid carriers, 800 μL of water and a drop of 1 M HCl. The lower organic phase was extracted, applied onto TLC plates, and resolved in organic solvents as described in the *Metabolic labeling studies* section. The fatty acid bands were scraped into scintillation vials and measured for radioactive contents. As a positive control for the assay, 10 μL of 0.05g/mL of Pancreatin was added to a separate reaction mixture containing McA pCIneo total membranes. (B), 20,000 dpm of [^{3}H]DG, prepared as described in *In ivtro DG hydrolase assay* in Chapter 2, was added to each sample mixture containing 90 μg of membrane proteins in 0.1 % CHAPS/PBS. The reaction mixture was incubated for 30 min at 37 °C. The reaction was stopped by the addition of 4 mL of chloroform/methanol 2:1 containing lipid carriers, 800 μL of water and a drop of 1 M HCl. The lower organic phase was extracted, applied onto TLC plates, and resolved in organic solvents as described in the *Metabolic labeling studies* section. The fatty acid bands were scraped into scintillation vials and measured for radioactive contents. As a positive control for the assay, 10 μL of 0.05g/mL of Pancreatin was added to a separate reaction mixture containing McA pCIneo membranes.

A
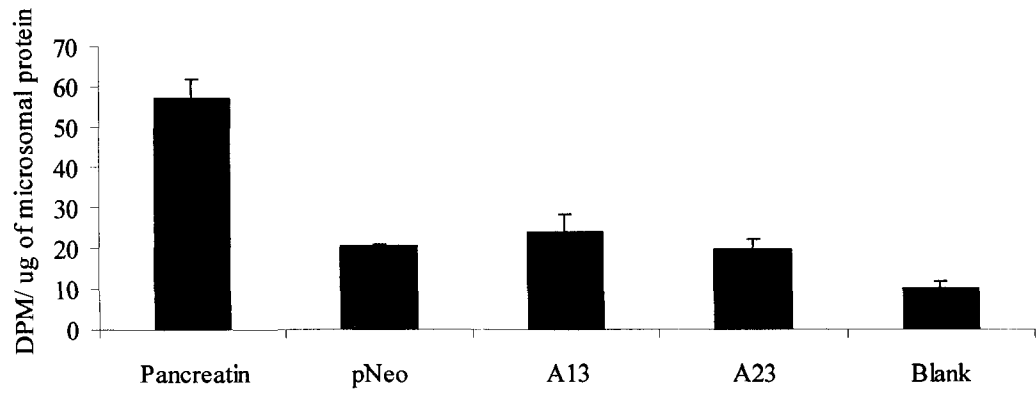
B
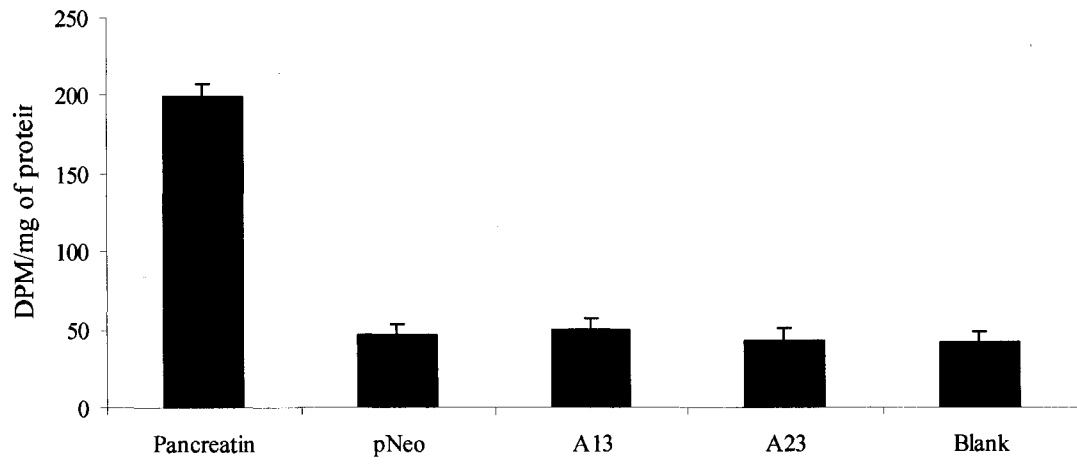
CHAPTER 5

SUMMARY AND FUTURE DIRECTIONS

5-1   Summary

Part I – Subcellular localization and membrane retention mechanism of mouse AADA

Integral membrane proteins that are destined to the Golgi, plasma membrane or endosomal compartments are inserted into the ER membrane, correctly folded and assembled, and then transported out of the ER along the secretory pathway (Schutze, 1994). While it is believed that specific signals are not required for directing proteins along the secretory pathway, protein targeting signals are shown to be crucial to retain proteins in specific organelles (Schutze, 1994). Such targeting and retention signals usually consist of short amino acid sequences located in the cytosolic domain of the protein (Schutze, 1994).

During translation, the signal peptide is recognized by a cytosolic RNA/protein complex known as the signal recognition particle (SRP) (Schatz, 1996). As the SRP binds the signal peptide, the SRP arrests protein synthesis until it has facilitated transfer of the nascent polypeptide –ribosome complex to the translocation channel at the ER (Schatz, 1996). A critical step in the protein folding process is dependent on whether the signal peptide is removed (Mziaut, 1999). If the signal peptide is removed, the newly synthesized N-terminus is generally located in the lumen of the ER; whereas when the signal peptide is not removed, the resulting N-terminal hydrophobic segment may function as a membrane anchor to direct the transmembrane insertion of the newly made polypeptide (Mziaut, 1999). Membrane proteins with uncleaved signal peptide can have either cytosolic or luminal orientation, which depends on properties such as charge distribution and the length of the transmembrane domain (Gafvelin, 1997).

Mziaut *et* al (1999) claimed that the evolutionarily conserved tyrosine cluster is critical to luminal targeting of AADA and that deletion of this region resulted in the loss of ER localization. However, such deletion mutant may not represent a valid model since deletion of six residues in the 17-amino acid transmembrane domain resulted in a transmembrane segment that was too short for insertion into any membranes, hence the resultant cytosolic localization. In the present study, the tyrosine residues were replaced by structurally similar but non-polar phenylalanine residues in order to determine the importance of the tyrosine cluster. Results from mutagenesis experiments revealed that the tyrosine residues are indeed critical for ER targeting and retention since replacement of tyrosines by phenylalanines resulted in re-localization to the Golgi for the YF-TMD-eGFP construct, while YF-AADA-eGFP still remained in the ER. It is therefore postulated that the transmembrane domain of AADA contains sufficient information for ER targeting and retention, but additional factors are also involved in keeping AADA in the ER. Although evidence is not yet available, it is strongly speculated that AADA is retained in the ER by formation of oligomers. This mechanism is believed to enhance ER retention efficiency of AADA since it has previously been shown that the oligomeric state can affect ER retention efficiency of two proteins bearing an identical double-arginine motif in their N-terminus (Schutze, 1994). This is a conclusion from an observation in which the double-arginine sorting signal maintained the trimeric mutant Iip33 in the ER more efficiently than the dimeric recombinant transferrin receptor (TfR) that contained the same double-arginine motif (Schutze, 1994). If oligomerization indeed enhances the ER retention efficiency of AADA, it can also explain why increasing

transmembrane domain length by insertion of 8 valine/leucine residues only altered ER

localization of the VL-TMD-eGFP construct, but not the VL-AADA-eGFP construct.

Glycosidase treatment assays confirmed that mouse AADA is an N-linked

glycoprotein with high mannose content due to its sensitivity towards Endo H, a high

mannose carbohydrate glycosidase. The sensitivity of AADA to Endo H indicated that

the enzyme had not been exposed to Golgi mannosidases, which agrees with results from

confocal immunofluorescence microscopy and subcellular fractionation studies that

AADA is localized to the ER. Although properties within the transmembrane domain of

AADA such as polarity of the tyrosine residues and transmembrane domain length confer

ER retention characteristics, additional factors exist to further enhance ER targeting and

retention of this protein. The importance of ER localization of AADA puts emphasis on

its proposed role in hepatic lipid metabolism since the ER is the subcellular compartment

most active in this process.

Part II – Role of mouse AADA in hepatic lipid metabolism in McA cells

Increased flux of fatty acids to the liver from adipose tissue during fasting is a

physiologically important process. The fatty acids that enter the liver are either re-

esterified into TG stores, which supply substrates for the assembly of VLDL, or utilized

for β-oxidation. Both processes result in the provision of substrates that are used by other

tissues during food deprivation. Ketone bodies that are formed from β-oxidation supply

the brain with an energy source, and hepatic VLDL secretion provides fatty acids for

energy production in peripheral tissues. The majority of TG secreted with VLDL is

derived from intracellular hepatic TG stores through a process that involves lipolysis and

re-esterification (Wiggins *et al*, 1992; Yang *et al*, 1995; Lankester *et al*, 1998). Although the mobilization of TG for VLDL secretion may represent an important regulatory step, not much is known regarding the lipases responsible for this process. The well-studied adipose tissue lipase HSL is not appreciably expressed in the liver (Kraemer *et al*, 1993), and ectopic expression of this enzyme in hepatoma cell lines (Pease *et al*, 1999; Reid *et al*, 2008) as well as adenoviral hepatic overexpression in mice (Reid *et al*, 2008) resulted in increased mobilization of TG stores, but the released fatty acids were delivered to mitochondria for β-oxidation rather than for re-esterification and VLDL assembly. Although the recently identified adipose tissue lipase, ATGL, has a broader tissue expression profile, its hepatic expression is relatively low (Haemmerle *et al*, 2006). Moreover, the role of this enzyme in hepatic lipid metabolism remains unknown despite the detailed characterization of ATGL null mice (Haemmerle *et al*, 2006). ATGL is activated by a lipid droplet–binding protein, CGI-58 (Lass *et al*, 2006), and recent studies suggested that overexpression of CGI-58 in McA cells increased VLDL secretion (Brown *et al*, 2007). However, it is currently unclear whether the CGI-58-mediated effect is due to regulation of ATGL that may be expressed in these cells, or through another yet unidentified mechanism. Reid *et al* (2008) have also shown that overexpression of ATGL in McA cells as well as adenoviral hepatic overexpression in mice increased fatty acid oxidation. From the studies on overexpression of HSL (Pease *et al*, 1999) and ATGL (Reid *et al*, 2008) in hepatoma cell lines together with adenoviral hepatic overexpression of HSL and ATGL in mice (Reid *et al*, 2008), it became obvious that the localization of lipases may determine the fate of the lipolytic products. Thus, hydrolysis of TG stores by a cytosolic lipase such as HSL may channel the released fatty acids to

mitochondria for oxidation, while release of fatty acids in the ER could result in re-esterification of the lipolytic products by ER-localized acyltransferases to support VLDL production. To date, two potential ER-localized TG lipases have been identified, AADA and TGH. While a positive role of TGH in the hepatic VLDL assembly has been documented (Dolinsky *et al*, 2004; Lehner *et al*, 1999-A; Lehner *et al*, 1999-B; Gilham *et al*, 2003), very little was known about the function of AADA in the liver.

Given its sequence homology to active site residues of HSL, and its primary expression in organs responsible for lipid metabolism, AADA is hypothesized to have a role in hepatic lipid metabolism (Trickett *et al*, 2001). HSL can hydrolyze a vast array of carboxylester substrates, including TG, DG, CE as well as artificial esters (Fredrikson *et al*, 1981). Therefore, it was postulated that AADA could also hydrolyze various esters. This study has demonstrated that AADA exhibits hydrolytic activity against insoluble lipidic esters, and that cells expressing AADA cDNA have decreased cellular TG, but not cellular PC or CE levels. This suggests that AADA, unlike HSL, does not appear to possess cholesteryl ester hydrolase activity. Since CE synthesis, like that of TG, is dependent on excess supply of fatty acids, and AADA expressing cells have similar CE levels as control cells in the presence of exogenous fatty acid supply, it is suggested that AADA does not play a role in fatty acid uptake into cells. Addition of the general lipase inhibitor E600 ablated the difference in intracellular TG levels between AADA and control cell lines, which also suggests that the observed reduction in TG in AADA expressing cells is not due to reduced TG synthesis, but a result of increased hydrolysis.

Interestingly, the rate of turnover of intracellular TG was similar between AADA expressing and control cells, which is an indication that TG stored in cytoplasmic lipid

droplets is not utilized by AADA. Since cells expressing AADA accumulated less TG in the presence of exogenous OA, this raises the possibility that AADA could act on one or more steps within the glycerol-3-phosphate pathway of de novo glycerolipid synthesis (Figure 5-1). Given the fact that PC and TG syntheses share common precursors up to the penultimate DG step, it would be expected that the synthesis of both of these lipids would be affected (Figure 5-1). A possible explanation to why TG levels could be affected without changes in PC levels is that sufficient DG is produced to support the more critical PC synthesis, but not enough of this substrate is present to augment TG synthesis. Another possibility would be that rather than hydrolyzing carboxylic esters, AADA could function as a thioesterase and hydrolyzes acyl-CoA, an obligate acyl-donor in glycerolipid biosynthesis. However, membranes isolated from AADA expressing cells did not exhibit increased oleoyl-CoA hydrolytic activity compared with control membranes, suggesting that oleoyl-CoA is not a substrate for the enzyme. In addition, since the active site of AADA faces the ER lumen, and acyl-CoA is believed to be synthesized on the cytosolic side of the ER (Coleman et al, 2000), it is unlikely that acyl-CoA would cross the ER membrane and become accessible by AADA. It is therefore more likely that AADA acts on newly synthesized DG or TG present within the ER bilayer. This would be in concert with the homology of AADA with HSL as the latter enzyme has been shown to possess a robust DG lipase activity in addition to its ability to hydrolyze TG and CE (Haemmerle et al, 2002).

Reduction in intracellular TG levels in AADA expressing cells was accompanied by increased levels of fatty acid oxidation. This reveals a possible function of AADA in hydrolyzing newly synthesized lipid substrates to support fatty acid oxidation. As

β-oxidation

FA   FA

Cytosol

G-3-P   LPA   PA   PAP   DG   TG

GPAT   AGPAT

ER Lumen

?
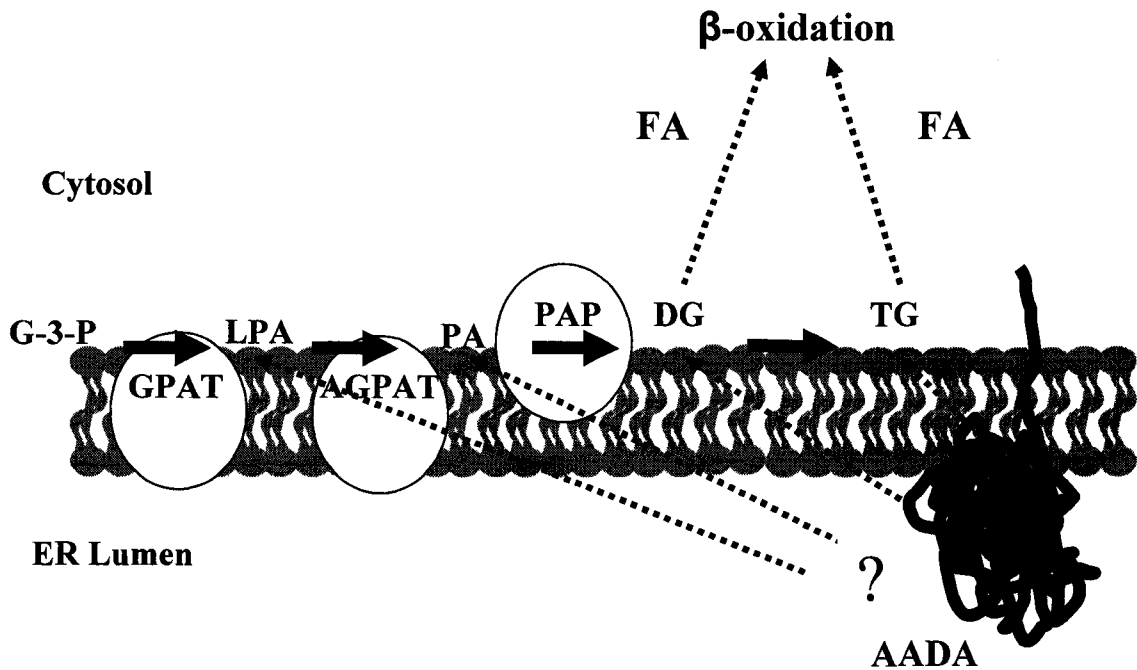
AADA

Figure 5-1. **The proposed role of AADA in the glycerol-3-phosphate pathway of TG synthesis and its effect on hepatic lipid metabolism.** AADA may act on one or more steps within the glycerol-3-phosphate pathway of de novo glycerolipid synthesis, which leads to hydrolysis of TG or the precursors of TG and PC synthesis. This could reflect the observed reduction in TG accumulation, while the fatty acids released from the glycerolipids are then destined to the mitochondria for β-oxidation. Due to its homology with HSL, primarily a DG lipase, it is possible that AADA also acts primarily on DG. Since PC levels are unaffected upon expression of AADA, it is speculated that sufficient DG is produced to support the necessary glycerophospholipid synthesis, but not enough of this substrate is present to augment TG synthesis. Abbreviations: AADA, arylacetamide deacetylase; AGPAT, 1-acylglycerol-3-phosphate acyltransferase; FA, fatty acids; G-3-P, glycerol-3-phosphate; GPAT, glycerol-3-phosphate acyltransferase; LPA, lysophosphatidic acid; PA, phosphatidic acid; PAP, phosphatidic acid phosphohydrolase/lipin.

suggested earlier, hydrolysis of TG stores by a lipase residing in or facing the cytosol may channel released fatty acids to mitochondria for oxidation, while release of fatty acids by lipases in or facing the ER could result in resterification of the lipolytic products by ER-localized acyltransferases for VLDL-TG secretion. Although the proposed function of AADA in releasing fatty acids for β-oxidation does not agree with its protein orientation in the ER membrane, the effect of its expression in McA cells parallels the effect of overexpression of HSL in McA cells, which was also shown to have reduced cellular TG levels that could be attributed to increased β-oxidation (Reid et al, 2008) Based on a 25 % sequence homology with HSL, it is not surprising that expression of both enzymes in McA cells has similar effects.

To address the discrepancy between topology of AADA within the ER membrane with its proposed function in hydrolyzing lipid substrates for fatty acid oxidation, it is believed that hydrolysis occurs at the ER membrane in which the enzymes of the glycerol-3-phosphate pathway for TG synthesis reside. Since AADA is a type II integral membrane protein, its active site and enzymatic activity are located near or at the ER membrane, and therefore, lipolytic products released at the ER membrane could preferentially diffuse across the membrane where they are directed to the mitochondria for β-oxidation instead of being re-esterified to TG for VLDL secretion. Despite of studies conducted by Debeer et al (1982) that suggested intracellular TG could provide substrates for fatty acid oxidation, a majority of the fatty acid comes from an extracellular source. This is supported by results demonstrated by Gibbons et al (1992), in which fatty acid oxidation levels were largely depended on extracellular fatty acid concentration and intracellular TG pools only had minor contributions. In agreement with the earlier

studies, AADA-mediated increase in fatty acid oxidation was only detected during the 4 hour pulse where there was presence of extracellular [^{3}H]OA, and this difference between AADA and control cells was lost during the 4 hour chase period when extracellular [^{3}H]OA was absent.

The decrease of cellular TG levels in AADA expressing cells was also accompanied by attenuated secretion of newly synthesized VLDL-TG. Results from this study appear to be in contrast to those reported by Gibbons *et al* (2000), who found that a HepG2 cell line expressing human AADA exhibited a 3-fold increase in TG secretion from intracellular stores during a 16 hour chase incubation (0.6 % of intracellular TG was secreted from control compared to 1.6 % from AADA cells); while in this study, the secretion of intracellular TG in both AADA cell lines is not different from control (about 0.7 % of intracellular TG was secreted during a 4 hour chase period in all lines). This difference cannot be explained by the inability of McA cells to deliver hydrolytic products for VLDL assembly because expression of TGH in McA cells resulted in increased lipidation of apoB100 and secretion of TG (Gilham *et al*, 2003; Kraemer *et al*, 2006).

In conclusion, our results indicate that expression of mouse AADA in McA cells, even at levels substantially below that present in the liver, decreases intracellular TG levels and VLDL-TG secretion, and hydrolytic products are destined to the mitochondria causing an increase in fatty acid oxidation levels. In addition, the ASM studies show that AADA-mediated enzymatic activity results in increased delivery of fatty acids derived from newly synthesized TG to the mitochondria, leading to approximately 20 % increase in fatty acid oxidation.

5-2   Future directions

Despite the presence of membrane targeting and retention properties of the transmembrane domain of mouse AADA, these characteristics are not crucial to membrane retention of the protein in the ER. Therefore, it is worthwhile to continue the investigation by focusing on the second proposed mechanism, oligomerization. The formation of large oligomeric structures is believed to prevent certain proteins of the ER to move forward through the secretory pathway, and by forming aggregation complexes either with itself or other ER resident proteins, this may prevent exit of AADA from the ER.

To demonstrate whether AADA exists as a monomer or multimer in its native state, cross-linking studies could be performed using the cross-linking reagent, dimethyl 3,3'-dithiobispropionimidate (DTBP). The purpose of using cross-linking reagents is to preserve any protein-protein interactions and prevent them from disruption during any biochemical manipulations. One method for identifying whether AADA forms oligomeric structures with itself is to co-transfect McA cells with two different tagged-AADA constructs, for example, FLAG-AADA and eGFP-AADA. Once McA cells are co-transfected with FLAG-AADA and eGFP-AADA, they can be treated with DTBP, and then subjected to standard immunoprecipitation procedures using anti-FLAG agarose beads. Following SDS-PAGE, immunoblotting with anti-eGFP antibodies would be able to identify the presence of any AADA complexes. Immunoblotting with antibodies against other ER resident membrane proteins such as calnexin could also reveal the existence of complexes with other proteins.

Initial studies on the function of mouse AADA showed that it has a role in hepatic lipid metabolism; however, the next objective would be to address if enhanced expression of AADA can promote similar effects *in vivo*. Infection of mice with adenovirus vectors containing cDNA of interest has been proven effective and is therefore proposed for further studies. A recombinant adenovirus carrying the mouse AADA gene will be delivered to mice by systemic administration, which is expected to target mainly to the liver. In addition to mouse AADA, the same procedure could be done using human AADA. Under both conditions, if the results obtained from McA cell lines truly reflect the physiological function of AADA, overexpression of both mouse and human AADA *in vivo* should lead to similar findings as in the cell lines. Besides studying the effects of protein overexpression *in vivo*, it is also necessary to consider employing short interfering RNA (siRNA) to knock-down AADA expression in mice to see if the opposite effects can be observed. Plasma and liver samples from AADA overexpressing and underexpressing mice can be collected for lipid analysis by gas chromatography. Hepatocytes can also be isolated to perform metabolic labeling studies similar to those performed in this thesis. In addition, the plasma collected can be fractionated by density gradient centrifugation to assess the lipidation state of secreted lipoproteins. If AADA-mediated hydrolysis of lipid substrates is impaired, the most prominent effect expected is that the supply of fatty acids to the mitochondria for β-oxidation will decrease in livers with no or low AADA activity, leading to lower fatty acid oxidation levels. As a result, hepatocytes isolated from AADA siRNA knock-down mice are speculated to accumulate higher levels of intracellular TG, hence more severe fatty liver condition. While there was no apparent disappearance of any lipids to indicate substrate specificity of AADA in

transfected McA cells, a comparison of lipid profiles of hepatocytes isolated from AADA overexpressing and underexpressing mice may reveal better information on this aspect. Since a complete ablation of the AADA gene in the siRNA knock-down approach is not guaranteed, this may not result in a phenotype that would provide clear answers with regards to AADA role in hepatic lipid metabolism. Therefore, an alternative approach to study the effects of the absence of AADA is to generate AADA knock-out mice. Based on the results obtained from AADA transfected McA cells, an adenoviral overexpression as well as a gene knock-down or knock-out of AADA seem to be studies that are worthwhile to consider, and any potential findings may provide insights into possible pharmacological interventions on lipid metabolic disorders.

References

Alam, M., D. Gilham, D.E. Vance, and R. Lehner. 2006. Mutation of F417 but not of L418 or L420 in the lipid binding domain decreases the activity of triacylglycerol hydrolase. *J Lipid Res*. 47:375-383.

Anelli, T., M. Alessio, A. Mezghrani, T. Simmen, F. Tamalo, A. Bachi, and R. Sitia. 2002. Erp44, a novel endoplasmic reticulum folding assistant of the thioredoxin family. *EMBO J.* 21:835-844.

Anelli, T., M. Alessio, A. Bachi, L. Bergamelli, G. Bertoli, S. Camerini, A. Mezghani, E. Ruffato, T. Simmen, and R. Sitia. 2003. Thiol-mediated protein retention in the endoplasmic reticulum: the role of Erp44. *EMBO J.* 22:5015-5022.

Boren, J., L. Graham, M. Wettesten, J. Scott, A. White, and S.O. Olofsson. 1992. The assembly and secretion of ApoB 100-containing lipoproteins in Hep G2 cells. ApoB 100 is cotranslationally integrated into lipoproteins. *J Biol Chem*. 267:9858-9867.

Brown, J.M., S. Chung, A. Das, G.S. Shelness, L.L. Rudel, and L. Yu. 2007. CGI-58 facilitates the mobilization of cytoplasmic triglyceride for lipoprotein secretion in hepatoma cells. *J Lipid Res*. 48:2295-2305.

Coleman, R.A., E.B. Haynes, T.M. Sand, and R.A. Davis. 1988. Developmental coordinate expression of triacylglycerol and small molecular weight apoB synthesis and secretion by rat hepatocytes. *J Lipid Res*. 29:33-42.

Coleman, R. A., Lewin, T. M., and Muoio, D. M. 2000. Physiological and nutritional regulation of enzymes of triacylglycerol synthesis. *Annu Rev Nutr.* 20: 77-103.

Coleman, R. A., and Lee, D. P. 2004. Enzymes of triacylglycerol synthesis and their regulation. *Prog Lipid Res.* 43:134-176.

Debeer, L. J., Beynen, A.C., Mannaerts, G. P., and Geelen, M. J. H. 1982. Lipolysis of hepatic triacylglycerol stores. *FEBS Lett.* 140:159-164.

Dolinsky, V.W., D. Gilham, M. Alam, D.E. Vance, and R. Lehner. 2004. Triacylglycerol hydrolase: role in intracellular lipid metabolism. *Cell Mol Life Sci.* 61:1633-1651.

Fisher, E.A., and H.N. Ginsberg. 2002. Complexity in the secretory pathway: the assembly and secretion of apolipoprotein B-containing lipoproteins. *J. Biol. Chem.* 277:17377-17380.

Folch, J., M. Lees, and G.H. Sloane Stanley. 1957. A simple method for the isolation and purification of total lipides from animal tissues. *J Biol Chem*. 226:497-509.

Francone, O. L., Kalopissis, A. D., and Griffaton, G. 1989. *Biochim Biophys Acta.* 1002:28-36.

Fredrikson, G., P. Stralfors, N.O. Nilsson, and P. Belfrage. 1981. Hormone-sensitive lipase of rat adipose tissue. Purification and some properties. *J Biol Chem.* 256:6311-6320.

Gafvelin, G., M. Sakaguchi, H. Andersson, and G. von Heijne. 1997. Topological rules for membrane protein assembly in eukaryotic cells. *J Biol Chem.* 272:6119-6127.

Gibbons, G.F., S.M. Bartlett, C.E. Sparks, and J.D. Sparks. 1992. Extracellular fatty acids are not utilized directly for the synthesis of very-low-density lipoprotein in primary cultures of rat hepatocytes. *Biochem J.* 287 (Pt 3):749-753.

Gibbons, G.F., K. Islam, and R.J. Pease. 2000. Mobilisation of triacylglycerol stores. *Biochim Biophys Acta.* 1483:37-57.

Gilham, D., M. Alam, W. Gao, D.E. Vance, and R. Lehner. 2005. Triacylglycerol hydrolase is localized to the endoplasmic reticulum by an unusual retrieval sequence where it participates in VLDL assembly without utilizing VLDL lipids as substrates. *Mol Biol Cell.* 16:984-996.

Gilham, D., S. Ho, M. Rasouli, P. Martres, D.E. Vance, and R. Lehner. 2003. Inhibitors of hepatic microsomal triacylglycerol hydrolase decrease very low density lipoprotein secretion. *Faseb J.* 17:1685-1687.

Gilham, D., and R. Lehner. 2005. Techniques to measure lipase and esterase activity in vitro. *Methods.* 36:139-147.

Grundy, S. M. 1990. Cholesterol and atherosclerosis: diagnosis and treatment. J. B. Lippincott Company, Philadelphia, PA.

Haemmerle, G., A. Lass, R. Zimmermann, G. Gorkiewicz, C. Meyer, J. Rozman, G. Heldmaier, R. Maier, C. Theussl, S. Eder, D. Kratky, E.F. Wagner, M. Klingenspor, G. Hoefler, and R. Zechner. 2006. Defective lipolysis and altered energy metabolism in mice lacking adipose triglyceride lipase. *Science.* 312:734-737.

Haemmerle, G., R. Zimmermann, J.G. Strauss, D. Kratky, M. Riederer, G. Knipping, and R. Zechner. 2002. Hormone-sensitive lipase deficiency in mice changes the plasma lipid profile by affecting the tissue-specific expression pattern of lipoprotein lipase in adipose tissue and muscle. *J Biol Chem.* 277:12946-12952.

Hansson, P.K., A.K. Asztely, J.C. Clapham, and S.A. Schreyer. 2004. Glucose and fatty acid metabolism in McA-RH7777 hepatoma cells vs. rat primary hepatocytes: responsiveness to nutrient availability. *Biochim Biophys Acta.* 1684:54-62.

Holm, C. 2003. Molecular mechanisms regulating hormone-sensitive lipase and lipolysis. *Biochem Soc Trans*. 31:1120-1124.

Jackson, M. R., Nilsson, T., and Peterson, P. A. 1990. Identification of a consensus motif for retention of transmembrane proteins in the endoplasmic reticulum. *EMBO J*. 9:3135-3162.

Kraemer, F.B., S. Patel, M.S. Saedi, and C. Sztalryd. 1993. Detection of hormone-sensitive lipase in various tissues. I. Expression of an HSL/bacterial fusion protein and generation of anti-HSL antibodies. *J Lipid Res*. 34:663-671.

Kraemer, F.B., and W.J. Shen. 2006. Hormone-sensitive lipase knockouts. *Nutr Metab (Lond)*. 3:12.

Kulinski, A., S. Rustaeus, and J.E. Vance. 2002. Microsomal triacylglycerol transfer protein is required for lumenal accretion of triacylglycerol not associated with ApoB, as well as for ApoB lipidation. *J Biol Chem*. 277:31516-31525.

Lankester, D.L., A.M. Brown, and V.A. Zammit. 1998. Use of cytosolic triacylglycerol hydrolysis products and of exogenous fatty acid for the synthesis of triacylglycerol secreted by cultured rat hepatocytes. *J Lipid Res*. 39:1889-1895.

Lass, A., R. Zimmermann, G. Haemmerle, M. Riederer, G. Schoiswohl, M. Schweiger, P. Kienesberger, J.G. Strauss, G. Gorkiewicz, and R. Zechner. 2006. Adipose triglyceride lipase-mediated lipolysis of cellular fat stores is activated by CGI-58 and defective in Chanarin-Dorfman Syndrome. *Cell Metab*. 3:309-319.

Lehner, R., Z. Cui, and D.E. Vance. 1999. Subcellullar localization, developmental expression and characterization of a liver triacylglycerol hydrolase. *Biochem J*. 338 (Pt 3):761-768.

Lehner, R., and D.E. Vance. 1999. Cloning and expression of a cDNA encoding a hepatic microsomal lipase that mobilizes stored triacylglycerol. *Biochem J*. 343 Pt 1:1-10.

Lehner, R., and R. Verger. 1997. Purification and characterization of a porcine liver microsomal triacylglycerol hydrolase. *Biochemistry*. 36:1861-1868.

Mitchell, D.M., M. Zhou, R. Pariyarath, H. Wang, J.D. Aitchison, H.N. Ginsberg, and E.A. Fisher. 1998. Apoprotein B100 has a prolonged interaction with the translocon during which its lipidation and translocation change from dependence on the microsomal triglyceride transfer protein to independence. *Proc Natl Acad Sci U S A*. 95:14733-14738.

Munro, S. 1995. An investigation on the role of transmembrane domains in Golgi protein retention. *EMBO J*. 14:4695-4704

Mziaut, H., Korza, G., Hand, A. R., Gerard, C., and Ozols, J. 1999. Targeting proteins to the lumen of endoplasmic reticulum using N-terminal domains of 11beta-hydroxysteroid dehydrogenase and the 50 kDa esterase. *J Biol Chem.* 274:14122-14129.

Olofsson, S.O., P. Stillemark-Billton, and L. Asp. 2000. Intracellular assembly of VLDL: two major steps in separate cell compartments. *Trends Cardiovasc Med.* 10:338-345.

Ozols, J. 1998. Determination of lumenal orientation of microsomal 50-kDa esterase/N-deacetylase. *Biochemistry.* 37:10336-10344.

Pease, R.J., D. Wiggins, E.D. Saggerson, J. Tree, and G.F. Gibbons. 1999. Metabolic characteristics of a human hepatoma cell line stably transfected with hormone-sensitive lipase. *Biochem J.* 341 (Pt 2):453-460.

Probst, M.R., M. Beer, D. Beer, P. Jeno, U.A. Meyer, and R. Gasser. 1994. Human liver arylacetamide deacetylase. Molecular cloning of a novel esterase involved in the metabolic activation of arylamine carcinogens with high sequence similarity to hormone-sensitive lipase. *J Biol Chem.* 269:21650-21656.

Raabe, M., M.M. Veniant, M.A. Sullivan, C.H. Zlot, J. Bjorkegren, L.B. Nielsen, J.S. Wong, R.L. Hamilton, and S.G. Young. 1999. Analysis of the role of microsomal triglyceride transfer protein in the liver of tissue-specific knockout mice. *J Clin Invest.* 103:1287-1298.

Reid, B.N., G.P. Ables, O.A. Otlivanchik, G. Schoiswohl, R. Zechner, W.S. Blaner, I.J. Goldberg, R.F. Schwabe, S.C. Chua, Jr., and L.S. Huang. 2008. Hepatic overexpression of hormone-sensitive lipase and adipose triglyceride lipase promotes fatty acid oxidation, stimulates direct release of free fatty acids, and ameliorates steatosis. *J Biol Chem.* 283:13087-13099.

Robbi, M., Beaufay, H. 1991. The COOH terminus of several liver carboxylesterases targets these enzymes to the lumen of the endoplasmic reticulum. *J Biol Chem.* 266: 20498-20503.

Rustaeus, S., P. Stillemark, K. Lindberg, D. Gordon, and S.O. Olofsson. 1998. The microsomal triglyceride transfer protein catalyzes the post-translational assembly of apolipoprotein B-100 very low density lipoprotein in McA-RH7777 cells. *J Biol Chem.* 273:5196-5203.

Schatz, G., and Dobberstein, B. 1996. Common principles of protein translocation across membranes. *Science.* 271: 1519-1526.

Schutze, M.P., P.A. Peterson, and M.R. Jackson. 1994. An N-terminal double-arginine motif maintains type II membrane proteins in the endoplasmic reticulum. *Embo J.* 13:1696-1705.

Tran, K., Thorne-Tjomsland, G., DeLong, C. J., Cui, Z., Shan, J., Burton, L., Jamieson, J. C., and Yao, Z. 2002. Intracellular assembly of very low density lipoproteins containing apolipoprotein B100 in rat hepatoma McA-RH7777 cells. *J Biol Chem.* 277:31187-31200.

Trickett, J.I., D.D. Patel, B.L. Knight, E.D. Saggerson, G.F. Gibbons, and R.J. Pease. 2001. Characterization of the rodent genes for arylacetamide deacetylase, a putative microsomal lipase, and evidence for transcriptional regulation. *J Biol Chem.* 276:39522-39532.

Wang, H., D. Gilham, and R. Lehner. 2007. Proteomic and lipid characterization of apolipoprotein B-free luminal lipid droplets from mouse liver microsomes: implications for very low density lipoprotein assembly. *J Biol Chem.* 282:33218-33226.

Wang, Y., K. Tran, and Z. Yao. 1999. The activity of microsomal triglyceride transfer protein is essential for accumulation of triglyceride within microsomes in McA-RH7777 cells. A unified model for the assembly of very low density lipoproteins. *J Biol Chem.* 274:27793-27800.

Wiggins, D., and G.F. Gibbons. 1992. The lipolysis/esterification cycle of hepatic triacylglycerol. Its role in the secretion of very-low-density lipoprotein and its response to hormones and sulphonylureas. *Biochem J.* 284 (Pt 2):457-462.

Yang, L.Y., A. Kuksis, J.J. Myher, and G. Steiner. 1995. Origin of triacylglycerol moiety of plasma very low density lipoproteins in the rat: structural studies. *J Lipid Res.* 36:125-136.

Yang, L.Y., A. Kuksis, J.J. Myher, and G. Steiner. 1996. Contribution of de novo fatty acid synthesis to very low density lipoprotein triacylglycerols: evidence from mass isotopomer distribution analysis of fatty acids synthesized from [2H6]ethanol. *J Lipid Res.* 37:262-274.

Yao, Z., and R.S. McLeod. 1994. Synthesis and secretion of hepatic apolipoprotein B-containing lipoproteins. *Biochim Biophys Acta.* 1212:152-166.

Zimmermann, R., J.G. Strauss, G. Haemmerle, G. Schoiswohl, R. Birner-Gruenberger, M. Riederer, A. Lass, G. Neuberger, F. Eisenhaber, A. Hermetter, and R. Zechner. 2004. Fat mobilization in adipose tissue is promoted by adipose triglyceride lipase. *Science.* 306:1383-1386.